

Fig. 4. Effects of the decreased level of Nrf2 on cell viability of CYP3A4-expressing HepG2 cells treated with the drugs. HepG2 cells were transfected with siNrf2 (●) or siScramble (○) at 10 nM for 24 h followed by infection with AdCYP3A4 at MOI 10 for 48 h. After cells were treated with six drugs for 24 h, WST-8 (A) and ATP (B) assays were performed for evaluation of the cell viability. Each point represents the mean \pm S.D. ($n = 3$). *, $P < 0.05$; **, $P < 0.01$; ***, $P < 0.001$, compared with AdCYP3A4-infected cells with siScramble in each concentration of drug.

of cellular stress, Nrf2 is localized in the cytosol by binding with Kelch-like erythroid cell-derived protein with CNC homology-associated protein 1. When cells are exposed to oxidative stress, the newly synthesized Nrf2 accumulates in the nucleus (Kobayashi et al., 2006). However, it has been reported that Nrf2 is localized in the nucleus in HepG2 cells under nonstressed conditions (Nguyen et al., 2005). In the present study, HepG2 cells with decreased Nrf2 expression were used to detect the drug-induced cytotoxicity more sensitively. The Nrf2 mRNA level in HepG2 cells could be decreased to less than 10% by siNrf2 (Fig. 3A). Given that the Nrf2 mRNA level in HepG2 was 1.6-fold higher than that in human hepatocytes (data not shown), the HepG2 cells used in this study had approximately 20% of the Nrf2 mRNA expression as that in human hepatocytes.

The present study was conducted as shown in Fig. 4 with four drugs (troglitazone, flutamide, acetaminophen, and clozapine) that did not show cytotoxicity in AdCYP3A4-infected HepG2 cells without siNrf2 and two drugs that did show cytotoxicity (desipramine and terbinafine). The viabilities of cells transfected with siNrf2 were significantly decreased by treatment with the drugs compared with those transfected with siScramble (Fig. 4). These results suggest that the

genes regulated by Nrf2 play important roles in the detoxification of the drug-induced cytotoxicities activated by CYP3A4. It has been reported that troglitazone is metabolized to quinone-type forms, which may be the reactive metabolites produced by CYP3A4 and CYP2C8 (Yamazaki et al., 1999). Although it has been reported that a postulated reactive metabolite of clozapine was produced by myeloperoxidase, leading to depletion of the cellular GSH level (Williams et al., 1997), there is no information about the association of CYP3A4 with the cytotoxicity of clozapine. Flutamide is reported to be oxidized into reactive metabolites that covalently bind to microsomal proteins metabolized by CYP3A4 and CYP1A2 (Berson et al., 1993; Fau et al., 1994). In addition, acetaminophen is metabolized to *N*-acetyl-*p*-benzoquinone imine, a postulated ultimate reactive metabolite, by CYP2E1 and CYP3A4 in humans. These reactive metabolites could be trapped with GSH in a process that is the major detoxification pathway. Because GCLC, GCLM, and glutathione peroxidase, which are important factors for maintaining the cellular GSH level, are regulated by Nrf2 (Thimmulappa et al., 2002), the decreased viability of AdCYP3A4-infected cells with siNrf2 by these drugs may be due to the decreased level of cellular GSH. The reactive metabolite of

terbinafine, TBF-A, is known to be trapped with GSH (Iverson and Uetrecht, 2001). The viability of AdCYP3A4-infected HepG2 cells was decreased by treatment with terbinafine even without siNrf2 transfection. This result was different from those by the treatment with troglitazone, flutamide, and acetaminophen. In addition, information about the association of CYP3A4/Nrf2 with desipramine-induced hepatotoxicity is limited, although epoxide formation and nitrosoalkane species were suggested to be related to the toxicity.

The WST-8 assay is a modified 3-(4,5-dimethylthiazol-2-yl)-2,5-diphenyl tetrazolium bromide assay, a conventional cytotoxicity assay, that uses a highly water-soluble disulfonated tetrazolium salt as a chromogenic indicator. The WST-8 assay was used to measure the mitochondrial NADH enzymes as an indicator of cell viability. The ATP assay was used to measure the cellular concentration of ATP, which is produced in mitochondria. Thus, in both assays, the cell viability was evaluated by measuring the mitochondrial activity, but the sensitivity of the ATP assay is lower than that of the WST-8 assay (Fig. 4), and the result should therefore be carefully evaluated.

Many researchers have used cells transfected with P450 expression plasmids to investigate the drug-induced cytotoxicity mediated by P450s, but this system generally could not induce high expression of P450 enzymes. However, our established adenovirus-using system induced the overexpression of CYP3A4 in HepG2 cells, resulting in more than 2.5-fold higher enzyme activity than that of human hepatocytes. In addition, the transfection of siNrf2 to HepG2 cells could decrease to approximately 20% the Nrf2 expression level in human hepatocytes. Thus, the combination of AdCYP3A4 infection with the transfection of siNrf2 would enable sensitive detection of the drug-induced cytotoxicity mediated by CYP3A4.

In conclusion, we constructed a highly sensitive cell-based system to detect the drug-induced cytotoxicity mediated by CYP3A4. Furthermore, we found that a decrease in the level of Nrf2 could increase the sensitivity of detection for drug-induced cytotoxicity. It is generally known that very complicated mechanisms are involved in drug-induced liver injury and the basic mechanism is likely to be different for different drugs. Therefore, this *in vitro* assay system is not likely to predict *in vivo* drug-induced liver injury. However, this system would be beneficial in the preclinical screening in drug development and increase our understanding of the drug-induced cytotoxicity associated with CYP3A4.

Acknowledgments

We thank Brent Bell for reviewing the manuscript.

Authorship Contributions

Participated in research design: Hosomi, Fukami, Nakajima, and Yokoi.

Conducted experiments: Hosomi and Iwamura.

Performed data analysis: Hosomi, Fukami, and Iwamura.

Wrote or contributed to the writing of the manuscript: Hosomi, Fukami, and Yokoi.

References

- Al-Kawas FH, Seeff LB, Berenson RA, Zimmerman HJ, and Ishak KG (1981) Allopurinol hepatotoxicity. Report of two cases and review of the literature. *Ann Intern Med* **95**:588–590.
- Aoyama T, Korzekwa K, Nagata K, Gillette J, Gelboin HV, and Gonzalez FJ (1990) Estradiol metabolism by complementary deoxyribonucleic acid-expressed human cytochrome P450s. *Endocrinology* **126**:3101–3106.
- Arellano F and Sacristán JA (1993) Allopurinol hypersensitivity syndrome: a review. *Ann Pharmacother* **27**:337–343.
- Balogun E, Hoque M, Gong P, Killen E, Green CJ, Foresti R, Alam J, and Motterlini R (2003) Curcumin activates the haem oxygenase-1 gene via regulation of Nrf2 and the antioxidant-responsive element. *Biochem J* **371**:887–895.
- Balson R, Gibson PR, Ames D, and Bhatl PS (1995) Tacrine-induced hepatotoxicity. Tolerability and management. *CNS Drugs* **4**:168–181.
- Beaune P, Dansette PM, Mansuy D, Kiffel L, Finck M, Amar C, Leroux JP, and Homberg JC (1987) Human anti-endoplasmic reticulum autoantibodies appearing in a drug-induced hepatitis are directed against a human liver cytochrome P-450 that hydroxylates the drug. *Proc Natl Acad Sci USA* **84**:551–555.
- Berson A, Wolf C, Chachaty C, Fisch C, Fau D, Eugene D, Loeper J, Gauthier JC, Beaune P, and Pompon D (1993) Metabolic activation of the nitroaromatic antiandrogen flutamide by rat and human cytochromes P-450, including forms belonging to the 3A and 1A subfamilies. *J Pharmacol Exp Ther* **265**:366–372.
- Boelsterli UA, Ho HK, Zhou S, and Leow KY (2006) Bioactivation and hepatotoxicity of nitroaromatic drugs. *Curr Drug Metab* **7**:715–727.
- Boelsterli UA and Lim PL (2007) Mitochondrial abnormalities—a link to idiosyncratic drug hepatotoxicity? *Toxicol Appl Pharmacol* **220**:92–107.
- Chan K, Han XD, and Kan YW (2001) An important function of Nrf2 in combating oxidative stress: detoxification of acetaminophen. *Proc Natl Acad Sci USA* **98**:4611–4616.
- Donato MT, Castell JV, and Gómez-Lechón MJ (1995) Effect of model inducers on cytochrome P450 activities of human hepatocytes in primary culture. *Drug Metab Dispos* **23**:553–558.
- Egnell AC, Houston B, and Boyer S (2003) *In vivo* CYP3A4 heteroactivation is a possible mechanism for the drug interaction between felbamate and carbamazepine. *J Pharmacol Exp Ther* **305**:1251–1262.
- Fau D, Eugene D, Berson A, Letteron P, Fromenty B, Fisch C, and Pessayre D (1994) Toxicity of the antiandrogen flutamide in isolated rat hepatocytes. *J Pharmacol Exp Ther* **269**:954–962.
- Gómez-Lechón MJ, Donato MT, Castell JV, and Jover R (2003) Human hepatocytes as a tool for studying toxicity and drug metabolism. *Curr Drug Metab* **4**:292–312.
- Gómez-Lechón MJ, Donato T, Jover R, Rodríguez C, Ponsoda X, Glaiese D, Castell JV, and Guignen-Guillouzo C (2001) Expression and induction of a large set of drug-metabolizing enzymes by the highly differentiated human hepatoma cell line BC2. *Eur J Biochem* **268**:1448–1459.
- Glue P, Banfield CR, Perhach JL, Mather GG, Racha JK, and Levy RH (1997) Pharmacokinetic interactions with felbamate. *In vitro-in vivo* correlation. *Clin Pharmacokinet* **33**:214–224.
- Guengerich FP (2008) Cytochrome P450 and chemical toxicology. *Chem Res Toxicol* **21**:70–83.
- Guengerich FP and MacDonald JS (2007) Applying mechanisms of chemical toxicity to predict drug safety. *Chem Res Toxicol* **20**:344–369.
- Hosomi H, Akai S, Minami K, Yoshikawa Y, Fukami T, Nakajima M, and Yokoi T (2010) An *in vitro* drug-induced hepatotoxicity screening system using CYP3A4-expressing and γ -glutamylcysteine synthetase knockdown cells. *Toxicol In Vitro* **24**:1032–1038.
- Huang YL, Chem HD, Su WJ, Wu JC, Chang SC, Chiang CH, Chang FY, and Lee SD (2003) Cytochrome P450 2E1 genotype and the susceptibility to anti-tuberculosis drug-induced hepatitis. *Hepatology* **37**:924–930.
- Iverson SL and Uetrecht JP (2001) Identification of a reactive metabolite of terbinafine: insights into terbinafine-induced hepatotoxicity. *Chem Res Toxicol* **14**:175–181.
- Kalutkar AS, Vaz AD, Lame ME, Henne KR, Soghia J, Zhao SX, Abramov YA, Lombardo F, Collin C, Hendsch ZS, et al. (2005) Bioactivation of the nontricyclic antidepressant nefazodone to a reactive quinone-imine species in human liver microsomes and recombinant cytochrome P450 3A4. *Drug Metab Dispos* **33**:243–253.
- Klatskin G (1975) Toxic and drug-induced hepatitis, in *Diseases of the Liver*, 4th ed (Schiff L ed) pp 604–710. JB Lippincott, Philadelphia.
- Kobayashi A, Kang MI, Watai Y, Tong KI, Shibata T, Uchida K, and Yamamoto M (2006) Oxidative and electrophilic stresses activate Nrf2 through inhibition of ubiquitination activity of Keap1. *Mol Cell Biol* **26**:221–229.
- Li AP, Lu C, Brent JA, Pham C, Fackett A, Ruegg CE, and Silber PM (1999) Cryopreserved human hepatocytes: characterization of drug-metabolizing enzyme activities and applications in higher throughput screening assays for hepatotoxicity, metabolic stability, and drug-drug interaction potential. *Chem Biol Interact* **121**:17–35.
- McCarthy TC, Pollak PT, Hanniman EA, and Sinal CJ (2004) Disruption of hepatic lipid homeostasis in mice after amiodarone treatment is associated with peroxisome proliferator-activated receptor- α target gene activation. *J Pharmacol Exp Ther* **311**:864–873.
- Mizuno K, Katoh M, Okumura H, Nakagawa N, Negishi T, Hashizume T, Nakajima M, and Yokoi T (2009) Metabolic activation of benzodiazepines by CYP3A4. *Drug Metab Dispos* **37**:345–351.
- Nakajima M, Itoh M, Sakai H, Fukami T, Katoh M, Yamazaki H, Kadlubar FF, Imaoka S, Funae Y, and Yokoi T (2006) CYP2A13 expressed in human bladder metabolically activates 4-aminobiphenyl. *Int J Cancer* **119**:2520–2526.
- Nakamura A, Nakajima M, Higashi E, Yamanaka H, and Yokoi T (2008) Genetic polymorphisms in the 5'-flanking region of human UDP-glucuronosyltransferase 2B7 affect the Nrf2-dependent transcriptional regulation. *Pharmacogenet Genomics* **18**:709–720.
- Nguyen T, Sherratt PJ, Nioi P, Yang CS, and Pickett CB (2005) Nrf2 controls constitutive and inducible expression of ARE-driven genes through a dynamic pathway involving nucleocytoplasmic shuttling by Keap 1. *J Biol Chem* **280**:32485–32492.
- Nioi P, McMahon M, Itoh K, Yamamoto M, and Hayes JD (2003) Identification of a novel Nrf2-regulated antioxidant response element (ARE) in the mouse NAD(P)H:quinone oxidoreductase 1 gene: reassessment of the ARE consensus sequence. *Biochem J* **374**:337–348.
- O'Brien PJ, Irwin W, Diaz D, Howard-Cofield E, Krejsa CM, Slaughter MR, Gao B, Kaludercic N, Angeline A, Bernardi P, et al. (2006) High concordance of drug-induced human hepatotoxicity with *in vitro* cytotoxicity measured in a novel cell-based model using high content screening. *Arch Toxicol* **80**:580–604.
- Ohbuchi M, Miyata M, Nagai D, Shimada M, Yoshinari K, and Yamazoe Y (2009) Role of enzymatic N-hydroxylation and reduction in flutamide metabolite-induced liver toxicity. *Drug Metab Dispos* **37**:97–105.
- Ohyama K, Nakajima M, Nakamura S, Shimada N, Yamazaki H, and Yokoi T (2000) A significant role of human cytochrome P450 2C8 in amiodarone N-deethylation: an approach to predict the contribution with relative activity factor. *Drug Metab Dispos* **28**:1303–1310.
- Osseni RA, Debbasch C, Christen MO, Rat P, and Warnet JM (1999) Tacrine-induced reactive oxygen species in a human liver cell line: the role of anethole dithiolethione as a scavenger. *Toxicol In Vitro* **13**:683–688.
- Smith KS, Smith PL, Heady TN, Trugman JM, Harman WD, and Macdonald TL (2003) *In vitro* metabolism of tolcapone to reactive intermediates: relevance to tolcapone liver toxicity. *Chem Res Toxicol* **16**:123–128.
- Thimmulappa RK, Mai KH, Srisuma S, Kensler TW, Yamamoto M, and Biswal S (2002) Identification of Nrf2-regulated genes induced by the chemopreventive agent sulforaphane by oligonucleotide microarray. *Cancer Res* **62**:5196–5203.
- Tsuchiya Y, Nakajima M, Kyo S, Kanaya T, Inoue M, and Yokoi T (2004) Human CYP1B1 is regulated by estradiol via estrogen receptor. *Cancer Res* **64**:3119–3125.

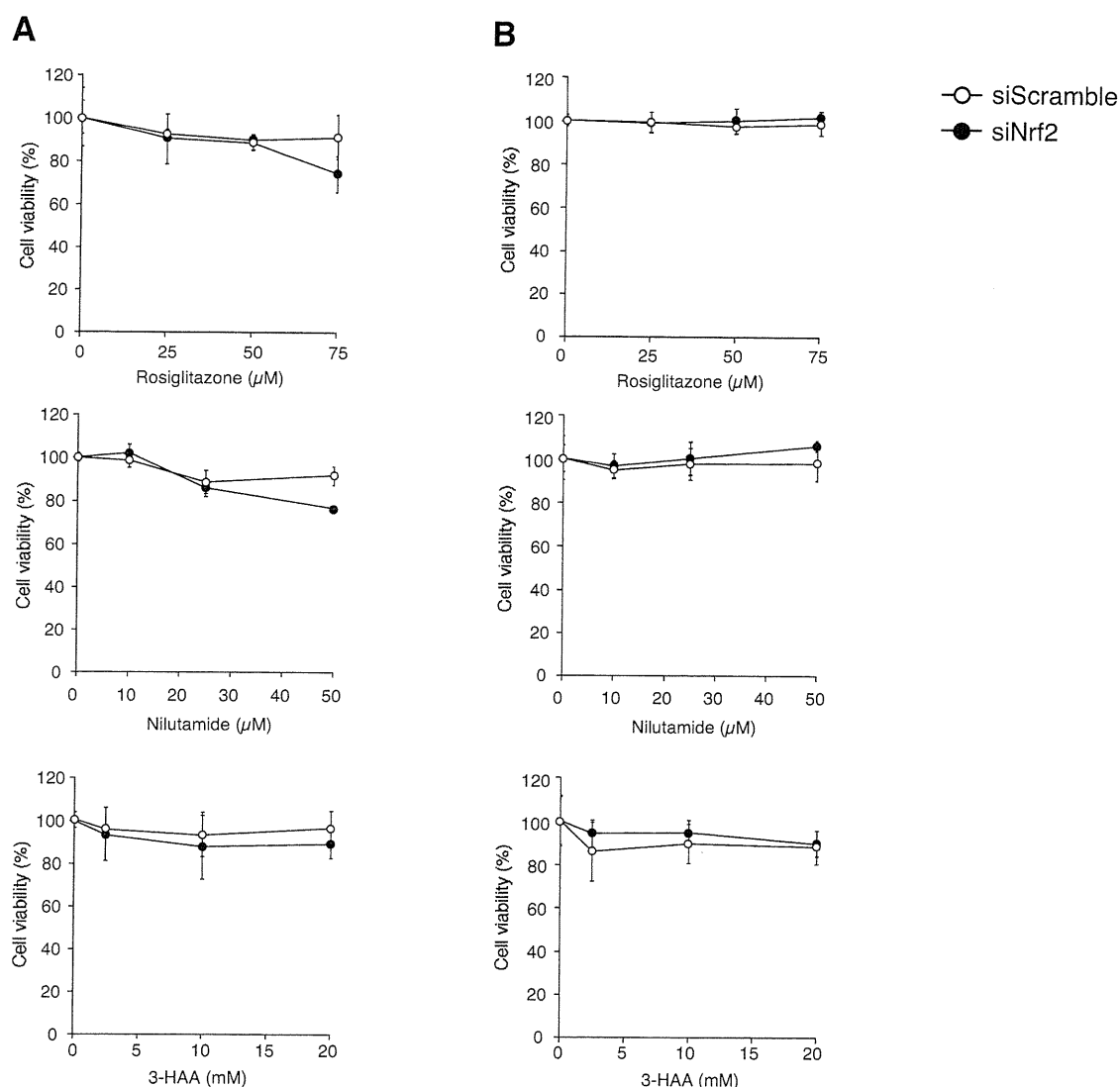
DMD

- Vignati L, Turlizzi E, Monaci S, Grossi P, Kanter R, and Monshouwer M (2005) An in vitro approach to detect metabolite toxicity due to CYP3A4-dependent bioactivation of xenobiotics. *Toxicology* **216**:154–167.
- Wang Y, Gray JP, Mishin V, Heck DE, Laskin DL, and Laskin JD (2008) Role of cytochrome P450 reductase in nitrofurantoin-induced redox cycling and cytotoxicity. *Free Radic Biol Med* **44**:1169–1179.
- Watkins PB (1992) Drug metabolism by cytochromes P450 in the liver and small bowel. *Gastroenterol Clin North Am* **21**:511–526.
- Westlind-Johnsson A, Malmebo S, Johansson A, Otter C, Andersson TB, Johansson I, Edwards RJ, Boobis AR, and Ingelman-Sundberg M (2003) Comparative analysis of CYP3A expression in human liver suggests only a minor role for CYP3A5 in drug metabolism. *Drug Metab Dispos* **31**:755–761.
- Williams DP, Pirmohamed M, Naisbitt DJ, Maggs JL, and Park BK (1997) Neutrophil cytotoxicity of the chemically reactive metabolite(s) of clozapine: possible role in agranulocytosis. *J Pharmacol Exp Ther* **283**:1375–1382.
- Xu JJ, Henstock PV, Dunn MC, Smith AR, Chabot JR, and de Graaf D (2008) Cellular imaging predictions of clinical drug-induced liver injury. *Toxicol Sci* **105**:97–105.
- Yamazaki H, Shibata A, Suzuki M, Nakajima M, Shimada N, Guengerich FP, and Yokoi T (1999) Oxidation of troglitazone to a quinone-type metabolite catalyzed by cytochrome P-450 2C8 and P-450 3A4 in human liver microsomes. *Drug Metab Dispos* **27**:1260–1266.
- Yoshikawa Y, Hosomi H, Fukami T, Nakajima M, and Yokoi T (2009) Establishment of knockdown of superoxide dismutase 2 and expression of CYP3A4 cell system to evaluate drug-induced cytotoxicity. *Toxicol In Vitro* **23**:1179–1187.
- Yoshitomi S, Ikemoto K, Takahashi J, Miki H, Namba M, and Asahi S (2001) Establishment of the transformants expressing human cytochrome P450 subtypes in HepG2, and their applications on drug metabolism and toxicology. *Toxicol In Vitro* **15**:245–256.
- Yun CH, Okerholm RA, and Guengerich FP (1993) Oxidation of the antihistaminic drug terfenadine in human liver microsomes. Role of cytochrome P-450 3A(4) in N-dealkylation and C-hydroxylation. *Drug Metab Dispos* **21**:403–409.

Address correspondence to: Dr. Tsuyoshi Yokoi, Drug Metabolism and Toxicology, Faculty of Pharmaceutical Sciences, Kanazawa University, Kakumamachi, Kanazawa 920-1192, Japan. E-mail: tyokoi@kenroku.kanazawa-u.ac.jp

Development of A High-sensitive Cytotoxicity Assay System for CYP3A4-mediated Metabolic Activation

Hiroko Hosomi, Tatsuki Fukami, Atsushi Iwamura, Miki Nakajima, and Tsuyoshi Yokoi
Drug Metab Dispos



Supplement Fig. S1: Effects of CYP3A4 expression and the decreased level of Nrf2 on cell viability of HepG2 cells treated with rosiglitazone, nilutamide, and 3-hydroxyacetanilide. HepG2 cells were transfected with siNrf2 (closed triangle) and siScramble (open triangle) at 10 nM for 24 hrs following by the infection with AdCYP3A4 at MOI 10 for 2 days. After cells were treated with drugs, (A) WST-8 and (B) ATP assays were performed for the evaluation of cell viability. Each data point represents mean \pm SD (n = 3).

Progesterone Receptor Membrane Component 1 Modulates Human Cytochrome P450 Activities in an Isoform-Dependent Manner^S

Shingo Oda, Miki Nakajima, Yasuyuki Toyoda, Tatsuki Fukami, and Tsuyoshi Yokoi

Drug Metabolism and Toxicology, Faculty of Pharmaceutical Sciences, Kanazawa University, Kakuma-machi, Kanazawa, Japan

Received May 26, 2011; accepted August 8, 2011

ABSTRACT:

Cytochromes P450 (P450s) catalyze the metabolism of a wide spectrum of compounds. Recently, progesterone receptor membrane component 1 (PGRMC1), which shares a key structural motif with cytochrome *b*₅, has been reported to bind to sterol- or steroid-synthesizing P450s, enhancing their activities. In this study, we investigated whether PGRMC1 affects human drug-metabolizing P450 activities. Using coexpression systems for PGRMC1 and P450s (CYP3A4, CYP2C9, or CYP2E1) in HepG2 cells, we found that PGRMC1 decreased the *V*_{max} values and increased the *K*_m values of the CYP3A4 activities, and it decreased the *V*_{max} values but did not affect the *K*_m values of the CYP2C9 activities. In contrast, PGRMC1 hardly affected the CYP2E1 activities. These results suggest that PGRMC1 negatively modulates the drug-metabolizing activities of P450, although it was isoform but not substrate de-

pendent. It is worth noting that coimmunoprecipitation analysis using coexpression systems for FLAG-PGRMC1 and Myc-P450s in human embryonic kidney 293 cells revealed that PGRMC1 interacts with all three P450s, although the affinity seemed to vary. In 29 human liver microsomes (HLMs), there was a 5-fold variability in the PGRMC1 protein levels. By the correlation analyses using the P450 activities and the PGRMC1 levels, we could neither observe the contribution of PGRMC1 to the P450 activities in HLMs nor that of the NADPH-cytochrome P450 reductase or cytochrome *b*₅. In conclusion, in contrast to sterol- or steroid-synthesizing P450s, we found that PGRMC1 negatively modulates the human drug-metabolizing activities of P450 through direct interaction. Further studies are needed to determine the clinical significance of PGRMC1 in the pharmacokinetics of drugs.

Introduction

Cytochrome P450 (P450) enzymes are heme-containing proteins that catalyze the metabolism of a wide variety of structurally diverse compounds (Nebert and Russell, 2002; Nelson et al., 2004). There are as many as 57 functional P450 genes and 58 pseudogenes in humans (<http://drnelson.utmem.edu/CytochromeP450.html>). Among them, three families, CYP1, CYP2, and CYP3, contribute to the oxidative metabolism of more than 70% of clinical drugs. Other P450 families (e.g., CYP4, CYP7, CYP11, CYP17, CYP19, CYP21, and CYP51) are involved in the metabolism of endogenous molecules such as steroids, bile acids, leukotrienes, and eicosanoids. P450 enzymes can exert their function by receiving electrons from NADPH-cytochrome P450 reductase (CPR) or cytochrome *b*₅ (Guengerich, 2002). CPR is indispensable for the P450 activities, whereas cytochrome *b*₅ has a significant role in the activities of some P450s (Shimada et al., 1994; Locuson et al., 2006).

Article, publication date, and citation information can be found at <http://dmd.aspetjournals.org>.

doi:10.1124/dmd.111.040907.

^S The online version of this article (available at <http://dmd.aspetjournals.org>) contains supplemental material.

Progesterone receptor membrane component 1 (PGRMC1) was originally identified as a membrane-associated nongenomic receptor for progesterone (Cahill, 2007). Although it is predominantly localized in endoplasmic reticulum, it seems to be detected in the plasma membrane, nucleus, and cytoplasm (Cahill, 2007; Lösel et al., 2008). PGRMC1 is widespread in eukaryotes from yeast to human. Despite its name, it is controversial whether progesterone binds to PGRMC1 (Min et al., 2005; Peluso et al., 2008b), and its function has not been fully understood. PGRMC1 is expressed in many tissues including liver, kidney, brain, breast, and adrenals (Cahill, 2007; Lösel et al., 2008). PGRMC1, a 22-kDa protein, contains a transmembrane domain at the N-terminal and a cytochrome *b*₅-like domain to which heme binds in the middle (Mifsud and Bateman, 2002; Min et al., 2004, 2005; Ghosh et al., 2005). For the association of PGRMC1 with the P450 activities, there are several reports as follows. Laird et al. (1988) reported that monoclonal antibody to rat inner zone antigen, a synonym of PGRMC1, blocked the 21-hydroxylation of progesterone in rat adrenal tissue. Min et al. (2005) reported that coexpression of PGRMC1, but not that of a heme-deficient PGRMC1 mutant, enhanced the human CYP21A2 activity in COS-7 cells. Hughes et al. (2007) demonstrated that damage associated protein 1, the yeast homolog of PGRMC1, binds and positively regulates CYP51A1 and

ABBREVIATIONS: P450, cytochrome P450; Ad, adenovirus; CPR, NADPH-cytochrome P450 reductase; GFP, green fluorescent protein; HLM, human liver microsomes; HPLC, high-performance liquid chromatography; MOI, multiplicity of infection; PGRMC1, progesterone receptor membrane component 1; HEK, human embryonic kidney; PCR, polymerase chain reaction; HCM, hepatocyte culture medium; PAGE, polyacrylamide gel electrophoresis; siRNA, small interfering RNA.

CYP61A1, which catalyze sterol biosynthesis, and knockdown of endogenous PGRMC1 in human embryonic kidney (HEK) 293 cells resulted in the decreased cholesterol synthesis catalyzed by human CYP51A1. Thus, it has been demonstrated that PGRMC1 positively regulates P450-mediated sterol or steroid syntheses, making it "a helping hand for P450 proteins" (Debose-Boyd, 2007).

In contrast to endobiotic-metabolizing P450s, there is limited information on the effects of PGRMC1 on xenobiotic-metabolizing P450s. Although it was shown, by coimmunoprecipitation using a coexpression system in HEK293 cells, that PGRMC1 bound to CYP3A4 (Hughes et al., 2007), the functional significance remains to be clarified. In this study, we sought to investigate whether PGRMC1 might be a regulator of human drug-metabolizing P450 activities, focusing on CYP3A4, CYP2C9, and CYP2E1.

Materials and Methods

Chemicals and Reagents. Testosterone was purchased from Wako Pure Chemical Industries (Osaka, Japan). 7-Ethoxycoumarin, 7-hydroxycoumarin, chlorzoxazone, 6-hydroxychlorzoxazone, diclofenac, and *S*-warfarin were from Sigma-Aldrich (St. Louis, MO). 4'-Hydroxydiclofenac, 6 β -hydroxytestosterone, and 7-hydroxywarfarin were purchased from BD Gentest (Woburn, MA), Steraloids (Newport, RI), and SAFC (St. Louis, MO), respectively. Midazolam and 1'-hydroxymidazolam were kindly provided by Astellas Pharmaceutical (Tokyo, Japan). Clonazepam was kindly provided by Roche Diagnostics (Basel, Switzerland). NADP⁺, glucose 6-phosphate, and glucose-6-phosphate dehydrogenase were from Oriental Yeast (Tokyo, Japan). The Adenovirus Expression Vector kit (Dual Version) and QuickTiter Adenovirus Titer Immunoassay kit were from Takara (Osaka, Japan) and Cell Biolabs (Tokyo, Japan), respectively. The pTARGET vector was purchased from Promega (Madison, WI). Lipofectamine 2000 was from Invitrogen (Carlsbad, CA). All primers were commercially synthesized at Hokkaido System Science (Sapporo, Japan). Rabbit anti-human CYP3A4 polyclonal antibody and rabbit anti-human CYP2C9 antibody were from BD Gentest. Goat anti-rat CYP2E1 polyclonal antibody was from Nossan (Yokohama, Japan). Rabbit anti-human PGRMC1 polyclonal antibody and mouse anti-FLAG monoclonal antibody (M2) were from Sigma-Aldrich. Rabbit anti-human/rat CPR antibody was from Millipore (Billerica, MA). Rabbit anti-cytochrome *b*₅ antibody and mouse anti-c-Myc monoclonal

antibody (9E10) were from Santa Cruz Biotechnology, Inc. (Santa Cruz, CA). Alexa Fluor 680 donkey anti-goat IgG was from Invitrogen. IRDye 680 goat anti-rabbit IgG and goat anti-mouse IgG were from LI-COR Biosciences (Lincoln, NE). All other chemicals and solvents were of the highest grade commercially available.

Construction of Recombinant Adenoviruses and Plasmids. Recombinant adenoviruses expressing CYP3A4 (AdCYP3A4), CYP2C9 (AdCYP2C9), and green fluorescent protein (AdGFP) were constructed as in our previous studies (Hosomi et al., 2010; Iwamura et al., 2011). Recombinant adenoviruses expressing PGRMC1 (AdPGRMC1) and CYP2E1 (AdCYP2E1) were created as follows. A fragment containing the full-length coding region of the human PGRMC1 or CYP2E1 cDNA was amplified by PCR using the primer pairs shown in Table 1 with a human liver cDNA as a template. The fragments were subcloned into the pAxCawit vector at a *Swa*I site. These vectors and the adenovirus genome DNA-terminal protein complex were cotransfected into HEK293 cells by Lipofectamine 2000. The recombinant adenovirus was isolated and propagated. Viral titers were determined using the QuickTiter Adenovirus Titer Immunoassay kit. The multiplicity of infection (MOI) was defined as the ratio of infectious units divided by the number of cells.

Expression vector for human PGRMC1 containing FLAG tag at the C terminus (FLAG-PGRMC1) was constructed as follows. Human PGRMC1 cDNA was amplified by PCR using the primers S-PGRMC1 and AS-FLAG PGRMC1 (Table 1) with the human liver cDNA as a template. The AS-FLAG PGRMC1 primer contains complementary sequences of FLAG tag and a stop codon. The PCR product was digested with *Bam*HI and *Xho*I and ligated into the pcDNA3.1 Hygro⁺ vector (Invitrogen).

Expression vectors for human P450s (CYP3A4, CYP2C9, and CYP2E1) containing 3 \times Myc tag at the C terminus (Myc-P450) were constructed as follows. Once P450 cDNA lacking a stop codon was amplified by PCR with the primer pairs shown in Table 1, it was digested with *Xho*I and *Kpn*I and subcloned into the pTARGET vector digested with the same restriction enzymes (pTARGET/P450 stop-). A double-strand DNA fragment containing three tandem copies of Myc tag sequence followed by a stop codon (Table 1) was subcloned into the pTARGET/P450 stop- plasmids digested with *Kpn*I and *Not*I. The nucleotide sequences of the constructed plasmids were confirmed by DNA sequencing analyses.

Cell Cultures. Human embryonic kidney cell line HEK293 and human hepatocellular carcinoma cell line HepG2 were obtained from American Type Culture Collection (Manassas, VA) and Riken Gene Bank (Tsukuba, Japan), respectively. These cells were cultured in Dulbecco's modified Eagle's me-

TABLE 1
Sequence of oligonucleotides used in this study

Oligonucleotide	5' to 3' Sequence
For construction of cosmid DNA	
S-PGRMC1	GAGTTCGGGATCCCTGCC ^a
AS-PGRMC1	ATACCTCGAGAGATATACTTCCACTG ^b
S-CYP2E1-1	ATGTCCTGCCCTCGGAGTCC
AS-CYP2E1-1	CTCATGAGCGGGGAATGACA
For construction of FLAG-tagged PGRMC1 plasmid	
S-PGRMC1	See above sequence
AS-FLAG PGRMC1	TAGACTCGAGCTACTTGTCTATCGTCTATCCTTGTAGTGCATATTTTCCGGGCACCT ^d
For construction of Myc-tagged P450 plasmids	
S-CYP3A4	TCACTCGAGATGGCTCTCATCCCAGACTTG ^{b,c}
AS-CYP3A4	CTCGGTACC ^c GGCTCCACTTACGGTGCCATC ^e
S-CYP2C9	TCACTCGAGATGGATTCTCTTGTGGTC ^{b,c}
AS-CYP2C9	CTCGGTACC ^c GACAGGAATGAAGCACAGC ^e
S-CYP2E1-2	TCACTCGAGATGTCTGCCCTCGGAGTCC ^{b,c}
AS-CYP2E1-2	CTCGGTACC ^c TGAGCGGGGAATGACACAGAG ^e
S-3 \times Myc	CTCGGTACCAGCAGAAAGCTGATCAGCGAGGAGGACCTGGAGCAGAAGCTGATCAGCG AGGAGGACCTGGAGCAGAAAGCTGATCAGCGAGGAGGACCTG7GAGCGGCCGCTCGACAG ^f CTGTCGACCGGGCCGCTCACAGGTCCTCTCGCTGATCAGCTTCTGTCTCCAGGTCC TCTCTGCTGATCAGCTTCTGTCTCCAGGTCTCTCTGCTGATCAGCTTCTGTCTCGGTACCGAG ^g
AS-3 \times Myc	

S, sense; AS, antisense.

^a The *Bam*HI site is underlined.

^b The *Xho*I site is underlined.

^c The start codon is in bold.

^d The *Xho*I site is underlined. Complementary sequences of FLAG tag are in bold. Complementary sequences of stop codon (TAG) are italicized.

^e The *Kpn*I site is underlined. The deleted stop codon is shown with the inverted caret.

^f The *Kpn*I and *Not*I sites are underlined. Three tandem Myc tags are in bold. The stop codon (TGA) is italicized.

^g The *Not*I and *Kpn*I sites are underlined. Complementary sequences of three tandem Myc tags are in bold. Complementary sequences of stop codon (TGA) are italicized.

dium (Nissui, Tokyo, Japan) supplemented with 0.1 mM nonessential amino acid (Invitrogen) and 10% fetal bovine serum (Invitrogen). For the construction of the coexpression systems for FLAG-PGRMC1 and Myc-P450, the HEK293 cells were cultured in Dulbecco's modified Eagle's medium containing 4.5 g/l glucose, 10 mM HEPES, and 10% fetal bovine serum. Human cryopreserved hepatocytes, lot H704 (Caucasian, female, 49 years old), were purchased from XenoTech, LLC (Lenexa, KS). The hepatocytes were cultured in hepatocyte culture medium (HCM) (Cambrex, East Rutherford, NJ) on a plate coated with Cell Matrix Type I-C (Nitta Gelatin, Tokyo, Japan). These cells were maintained at 37°C under an atmosphere of 5% CO₂, 95% air.

Infection of Recombinant Adenoviruses to HepG2 Cells or Cryopreserved Human Hepatocytes. HepG2 cells were seeded at 7.5×10^5 cells/well into a six-well plate and were allowed to grow confluent. The cells were infected with a constant MOI of AdCYP (AdCYP3A4, 5; AdCYP2C9, 20; AdCYP2E1, 25; represented as $\times 1$ in Fig. 1) and varied MOI of AdPGRMC1 (0, 2.5, 5, and 10 represented as 0, $\times 1$, $\times 2$, and $\times 4$, respectively). To make the total MOI the same value in four different experimental conditions, AdGFP was infected. After 24 h, the cultured medium was replaced with fresh medium without adenovirus. After 48 h, total cell homogenates were prepared by homogenization with TGE buffer (10 mM Tris-HCl, pH 7.4, 20% glycerol, and 0.1 mM EDTA). The protein concentration was determined using Bradford protein assay reagent (Bio-Rad Laboratories, Hercules, CA) with γ -globulin as a standard.

The human hepatocytes were seeded at 1.5×10^6 cells/well into a 6-well plate. After 3 h, the medium was changed to HCM (albumin and antibiotics free) containing AdPGRMC1 or AdGFP at MOI 30. After 1 h, the medium was replaced with fresh HCM. After 48 h, the total cell homogenates were prepared as described above.

Human Liver Microsomes. Pooled human liver microsomes (HLMs) ($n = 50$) and individual HLMs (20 donors) were purchased from BD Gentest. Human liver samples from nine donors were obtained from the Human and Animal Bridging Research Organization (Chiba, Japan), which is in partnership with the National Disease Research Interchange (Philadelphia, PA). Microsomes were prepared according to the method described previously (Tabata et al., 2004).

SDS-Polyacrylamide Gel Electrophoresis and Western Blotting. Total cell homogenates or HLMs (20 μ g) were separated with 10% SDS-polyacrylamide gel electrophoresis (PAGE) for the detection of P450s and with 15% SDS-PAGE for the detection of PGRMC1. The separated proteins were electrotransferred onto the polyvinylidene difluoride membrane Immobilon-P (Millipore). The membranes were probed with rabbit anti-human CYP3A4, goat anti-rat CYP2E1, rabbit anti-human CYP2C9, rabbit anti-human PGRMC1, anti-human/rat CPR, or anti-cytochrome *b*₅ antibodies and the corresponding fluorescent dye-conjugated secondary antibodies. The band densities were quantified with the Odyssey Infrared Imaging system (LI-COR Biosciences). The expression levels of P450 proteins were defined on the basis of a standard curve using P450 Supersomes (BD Gentest).

Enzyme Assays. A typical incubation mixture (final volume, 0.2 ml) contained 0.4 mg/ml total cell homogenate or 0.2 mg/ml HLM, 100 mM potassium phosphate buffer, pH 7.4, an NADPH-generating system (0.5 mM NADP⁺, 5 mM glucose 6-phosphate, 5 mM MgCl₂, and 1 unit/ml glucose 6-phosphate dehydrogenase), and each substrate. The reaction mixture was

preincubated at 37°C for 2 min, and the reaction was started by adding the NADPH-generating system.

The testosterone 6 β -hydroxylase activity was determined as described previously (Nakajima et al., 1999) with a 20-min reaction time. The product formation was determined using HPLC with a LachromUltra C18 column (4.6 \times 100 mm; 3 μ m; Hitachi, Tokyo, Japan) and monitored at 240 nm.

The midazolam 1'-hydroxylase activity was determined as described previously (Kronbach et al., 1989) with slight modifications. The reaction mixture was incubated at 37°C for 15 min, and the reaction was terminated by adding 100 μ l of ice-cold methanol. Clonazepam (20 ng) was added as an internal standard. After the removal of the protein by centrifugation at 10,000g for 5 min, a 20- μ l portion of the sample was subjected to a liquid chromatography-tandem mass spectrometry system with an HP 1100 system including a binary pump, an automatic sampler, and a column oven (AB Sciex, Tokyo, Japan), which was equipped with a ZORBAX SB-C18 column (2.1 \times 50 mm; 3.5 μ m; Agilent Technologies). The column temperature was 20°C, and the flow rate was 0.2 ml/min. The mobile phase was 0.1% formic acid in water (A) and 0.1% formic acid in acetonitrile (B). A linear gradient was used from 20% B to 90% B over 2 to 3 min followed by 90% B for 7 min, and then the column was allowed to re-equilibrate at the initial conditions for 4 min. The liquid chromatography was connected to a PE Sciex API 2000 tandem mass spectrometer (AB Sciex) operated in the positive electrospray ionization mode. The turbo gas was maintained at 550°C. Nitrogen was used as the nebulizing gas, turbo gas, and curtain gas at 40, 90, and 40 psi, respectively. Parent and/or fragment ions were filtered in the first quadrupole and dissociated in the collision cell using nitrogen as the collision gas. The collision energy was 37 V. The mass/charge (*m/z*) ion transitions were recorded in the multiple reaction monitoring mode: *m/z* 342.0 and 203.0 for 1'-hydroxymidazolam; *m/z* 315.9 and 270.1 for clonazepam.

The *S*-warfarin 7-hydroxylase activity was determined as described previously (Yamazaki et al., 1997) with a 20-min incubation time. The product formation was determined using HPLC with a Mightysil RP-18 column (4.6 \times 150 mm; 5 μ m; Kanto Chemical, Tokyo, Japan) and monitored with the excitation wavelength set at 320 nm and the emission set at 415 nm.

The diclofenac 4'-hydroxylase activity was determined by the method used by Katoh et al. (2004) with a 30-min incubation time. The product formation was determined using HPLC with a TSK-GEL ODS-80T_M column (4.6 \times 250 mm; 5 μ m; TOSOH, Tokyo, Japan) and monitored at 280 nm.

The chlorzoxazone 6-hydroxylase activity was determined as described previously (Mohri et al., 2010) with a 30-min incubation time. The product formation was determined using HPLC with a LachromUltra C18 column (4.6 \times 100 mm; 3 μ m) and monitored at 295 nm.

The 7-ethoxycoumarin *O*-deethylase activity was determined as described previously (Yamazaki et al., 1999) with a 30-min incubation time. The product formation was determined using HPLC with a Mightysil RP-18 column (4.6 \times 150 mm; 5 μ m) and monitored with the excitation wavelength set at 338 nm and the emission set at 458 nm.

Kinetic parameters were estimated from the fitted curve using a computer program (KaleidaGraph; Synergy Software, Reading, PA) designed for non-linear regression analysis. The following equations were used: Michaelis-Menten equation, $V = V_{\max} \times [S]/(K_m + [S])$; and substrate inhibition equation, $V = V_{\max} \times [S]/(K_m + S + [S]^2/K_i)$, where V is the velocity of the

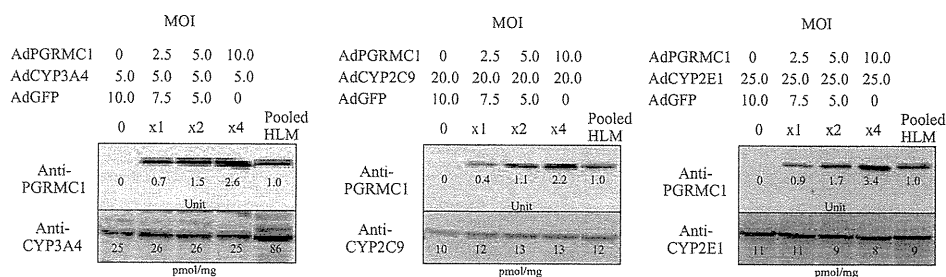


Fig. 1. Establishment of coexpression systems for PGRMC1 and CYP3A4, CYP2C9, or CYP2E1. HepG2 cells were infected with AdPGRMC1, each AdP450, and AdGFP for 72 h at the indicated MOI. Total MOI was adjusted by the infection of AdGFP. Twenty micrograms of total cell homogenates from the HepG2 or human liver microsomes were subjected to Western blot analyses. The absolute P450 protein levels were determined using a standard curve with each human P450 Supersome. The PGRMC1 protein levels were expressed relative to the value in the pooled HLMs set at 1.0. The values on the membrane are the mean of two independent determinations.

reaction, $[S]$ is the substrate concentration, K_m is the Michaelis-Menten constant, V_{max} is the maximum velocity, and K_i is the substrate inhibition constant. Data are expressed as the means \pm S.D. of three independent determinations.

Coimmunoprecipitation Assay. The FLAG-PGRMC1 and each Myc-P450 expression plasmid were transiently cotransfected into HEK293 cells. In brief, the day before transfection, the cells were seeded into a six-well plate coated with Cell Matrix Type I-C. After 24 h, each 2 μ g of FLAG-PGRMC1 and Myc-P450 plasmids was transfected using Lipofectamine 2000. After 48 h, the cells were collected, and total cell homogenates were prepared by homogenization with TGE buffer. Five hundred micrograms of protein were suspended in either buffer A or buffer B in a final volume of 0.5 ml and rotated at 4°C for 2 h. Buffer A consisted of 0.5% Nonidet P-40, 0.25% sodium deoxycholate, 50 mM Tris-HCl, pH 7.4, 150 mM NaCl, 1 mM EDTA, 0.5 mM (*p*-aminodiphenyl)-methanesulfonyl fluoride hydrochloride, 2 μ g/ml aprotinin, and 2 μ g/ml leupeptin. The detergents in buffer A were replaced with 0.1% digitonin in buffer B. The lysates were centrifuged at 100,000g for 30 min. To the supernatants, the anti-FLAG antibody was added and incubated for 8 h followed by precipitation with protein G-Sepharose beads. The beads were washed with buffer A or B and suspended with Laemmli sample buffer. The eluent was subjected to Western blot analyses with anti-FLAG antibody or anti-c-Myc antibody.

Statistical Analyses. Statistical significance was determined by using an unpaired, two-tailed Student's *t* test for paired data between two groups or the Shirley-Williams' test when more than three groups were compared. Correlation analyses were performed by Pearson's product-moment method. When the *P* value was less than 0.05, the differences were considered statistically significant.

Results

Establishment of Coexpression Systems for PGRMC1 and P450s in HepG2 Cells. To establish coexpression systems for PGRMC1 and P450s, AdPGRMC1 was cotransfected with AdCYP3A4, AdCYP2C9, or AdCYP2E1 into the HepG2 cells. Preliminarily, we optimized the MOIs to obtain the expression levels of PGRMC1 and P450s that are close to those in pooled human liver microsomes. When AdPGRMC1 was infected at MOI 3 to 4, the expressed PGRMC1 levels were close to those in the pooled HLMs. Accordingly, we set the MOIs for AdPGRMC1 at 2.5, 5, and 10, which were represented as $\times 1$, $\times 2$, and $\times 4$, respectively (Fig. 1). The MOIs for AdCYP2C9 and AdCYP2E1 were set at 20 and 25, respectively. In the case of AdCYP3A4, MOIs over 10 showed cellular toxicity. Therefore, we set the MOIs for AdCYP3A4 at 5, although the level of CYP3A4 protein produced was lower than that in the pooled HLMs (Fig. 1) but was in the range of those in individual HLMs, as described below. Thus, we obtained four lines for each P450

with various levels of PGRMC1. Using these systems, we investigated the effects of PGRMC1 on the P450 activities.

Effects of Coexpression of PGRMC1 on CYP3A4 Activities. To investigate the effects of PGRMC1 on the CYP3A4 activity, kinetic analyses of testosterone 6 β -hydroxylation and midazolam 1'-hydroxylation were performed using the total cell homogenates from the HepG2 coexpression system. The kinetics of testosterone 6 β -hydroxylation followed the Michaelis-Menten equation (Fig. 2A). The K_m , V_{max} , and V_{max}/K_m values of the homogenates from the cells with no exogenous PGRMC1 were $56.9 \pm 9.1 \mu\text{M}$, $54.3 \pm 4.0 \text{ pmol} \cdot \text{min}^{-1} \cdot \text{pmol P450}^{-1}$, and $0.96 \pm 0.08 \mu\text{l} \cdot \text{min}^{-1} \cdot \text{pmol P450}^{-1}$, respectively (Table 2). The coexpression of PGRMC1 significantly decreased the V_{max} values and increased the K_m values, resulting in a decrease in the V_{max}/K_m values in a PGRMC1 concentration-dependent manner. The kinetics of midazolam 1'-hydroxylation followed the substrate-inhibition equation (Fig. 2B). The K_m , V_{max} , K_i , and V_{max}/K_m values by the homogenates from the cells with no exogenous PGRMC1 were $5.7 \pm 0.9 \mu\text{M}$, $9.8 \pm 1.5 \text{ pmol} \cdot \text{min}^{-1} \cdot \text{pmol P450}^{-1}$, $15.9 \pm 4.1 \mu\text{M}$, and $1.72 \pm 0.03 \mu\text{l} \cdot \text{min}^{-1} \cdot \text{pmol}^{-1} \text{ P450}$, respectively (Table 2). The coexpression of PGRMC1 significantly decreased the V_{max} values and increased the K_m values, resulting in a decrease in the V_{max}/K_m values in a PGRMC1 concentration-dependent manner. The K_i value was not affected by the coexpression of PGRMC1. Thus, it was demonstrated that PGRMC1 has the ability to attenuate the CYP3A4 activity independently of the substrate.

Effects of Coexpression of PGRMC1 on CYP2C9 Activities. To investigate the effects of PGRMC1 on the CYP2C9 activity, kinetic analyses of *S*-warfarin 7-hydroxylation and diclofenac 4'-hydroxylation were performed. The kinetics of *S*-warfarin 7-hydroxylation followed the Michaelis-Menten equation (Fig. 3A). The K_m , V_{max} , and V_{max}/K_m values by the homogenates from the cells with no exogenous PGRMC1 were $1.6 \pm 0.1 \mu\text{M}$, $5.4 \pm 0.2 \text{ pmol} \cdot \text{min}^{-1} \cdot \text{pmol P450}^{-1}$, and $3.3 \pm 0.2 \mu\text{l} \cdot \text{min}^{-1} \cdot \text{pmol P450}^{-1}$, respectively (Table 3). The coexpression of PGRMC1 significantly decreased the V_{max} values in a PGRMC1 concentration-dependent manner but did not affect the K_m values, resulting in a decrease in the V_{max}/K_m values. The kinetics of diclofenac 4'-hydroxylation followed the Michaelis-Menten equation (Fig. 3B). The K_m , V_{max} , and V_{max}/K_m values by the homogenates from the cells with no exogenous PGRMC1 were $7.3 \pm 0.3 \mu\text{M}$, $91.6 \pm 6.8 \text{ pmol} \cdot \text{min}^{-1} \cdot \text{pmol P450}^{-1}$, and $12.6 \pm 1.5 \mu\text{l} \cdot \text{min}^{-1} \cdot \text{pmol P450}^{-1}$, respectively (Table 3). The coexpression of PGRMC1

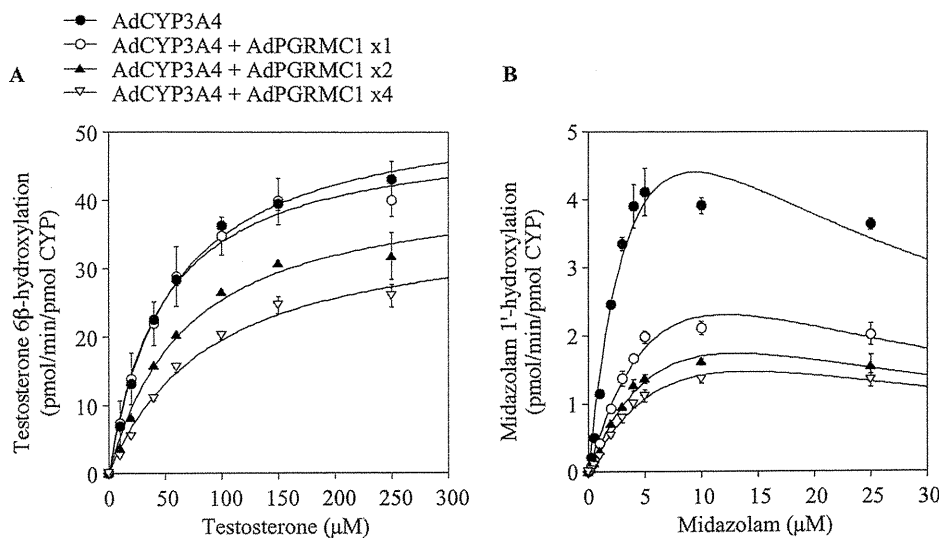


FIG. 2. Kinetic analyses of testosterone 6 β -hydroxylation (A) and midazolam 1'-hydroxylation (B) by recombinant CYP3A4 in single or coexpression systems with PGRMC1. The expression systems were constructed using recombinant adenoviruses as described under *Materials and Methods*. The obtained kinetic parameters are shown in Table 2. Data are the means \pm S.D. of three independent determinations.

TABLE 2

Kinetic parameters for testosterone 6 β -hydroxylase activity and midazolam 1'-hydroxylase activity by recombinant CYP3A4 in single or coexpression systems with PGRMC1

The expression systems were constructed using recombinant adenoviruses as described under *Materials and Methods*. Kinetic parameters were calculated from curves by nonlinear regression. Data are mean \pm S.D. of three independent experiments.

AdCYP3A4 + AdPGRMC1	Testosterone 6 β -Hydroxylation			Midazolam 1'-Hydroxylation			
	K_m μM	V_{max} $pmol \cdot min^{-1} \cdot pmol P450^{-1}$	V_{max}/K_m $\mu l \cdot min^{-1} \cdot pmol P450^{-1}$	K_m μM	V_{max} $pmol \cdot min^{-1} \cdot pmol P450^{-1}$	K_i μM	V_{max}/K_m $\mu l \cdot min^{-1} \cdot pmol P450^{-1}$
	56.9 \pm 9.1	54.3 \pm 4.0	0.96 \pm 0.08	5.7 \pm 0.9	9.8 \pm 1.5	15.9 \pm 4.1	1.72 \pm 0.03
$\times 1$	53.1 \pm 22.3	51.2 \pm 5.9	1.07 \pm 0.42	10.9 \pm 2.2*	6.5 \pm 0.7*	10.4 \pm 7.5	0.60 \pm 0.05*
$\times 2$	71.4 \pm 14.2	43.4 \pm 4.4*	0.62 \pm 0.07*	11.6 \pm 3.8*	5.0 \pm 1.4*	17.8 \pm 11.6	0.44 \pm 0.04*
$\times 4$	91.8 \pm 12.2*	37.4 \pm 2.7**	0.41 \pm 0.04*	12.5 \pm 2.1*	4.1 \pm 0.6**	16.3 \pm 3.1	0.33 \pm 0.01**

* $P < 0.05$ and ** $P < 0.01$ compared with control by Shirley-Williams' test.

significantly decreased the V_{max} values in a PGRMC1 concentration-dependent manner but did not affect the K_m values, resulting in a decrease in the V_{max}/K_m values. Thus, it was demonstrated that PGRMC1 has the ability to attenuate the CYP2C9 activity independently of the substrate.

Effects of Coexpression of PGRMC1 on CYP2E1 Activities. To investigate the effects of PGRMC1 on the CYP2E1 activity, kinetic analyses of chlorzoxazone 6-hydroxylation and 7-ethoxycoumarin O-deethylation were performed. The kinetics of chlorzoxazone 6-hydroxylation followed the Michaelis-Menten equation (Fig. 4A). The K_m , V_{max} , and V_{max}/K_m values by the homogenates from the cells with no exogenous PGRMC1 were 67.1 \pm 5.6 μM , 618.3 \pm 18.2 $pmol \cdot min^{-1} \cdot pmol P450^{-1}$, and 9.3 \pm 0.5 $\mu l \cdot min^{-1} \cdot pmol P450^{-1}$, respectively (Table 4). The coexpression of PGRMC1 did not affect the kinetic parameters. The kinetics of 7-ethoxycoumarin O-deethylation followed the Michaelis-Menten equation (Fig. 4B). The K_m , V_{max} , and V_{max}/K_m values by the homogenates from the cells with no exogenous PGRMC1 were 40.2 \pm 2.5 μM , 16.0 \pm 1.2 $pmol \cdot min^{-1} \cdot pmol P450^{-1}$, and 0.40 \pm 0.01 $\mu l \cdot min^{-1} \cdot pmol P450^{-1}$, respectively (Table 4). The coexpression of PGRMC1 did not affect the K_m and V_{max} values but slightly decreased the V_{max}/K_m values. PGRMC1 likely had a small effect on the CYP2E1 activities in comparison with the CYP3A4 and CYP2C9.

Effects of Overexpression of PGRMC1 on Enzyme Activities in Human Hepatocytes. To investigate whether PGRMC1 modulates the activities of endogenous human P450s, we sought to overexpress PGRMC1 in human hepatocytes. When the homogenates from the

human hepatocytes were subjected to Western blot analysis, the band density of PGRMC1 protein was similar to that in the pooled HLMs (Fig. 5A). When AdPGRMC1 was infected, the PGRMC1 protein level was significantly (5.6-fold, $P < 0.001$) increased (Fig. 5A). We confirmed that there was no morphological change by the infection with AdPGRMC1. Using the homogenates from these cells, the midazolam 1'-hydroxylase, *S*-warfarin 7-hydroxylase, and chlorzoxazone 6-hydroxylase activities, at the substrate concentrations of 10, 10, and 500 μM , respectively, were evaluated. Interestingly, we found that the midazolam 1'-hydroxylase and *S*-warfarin 7-hydroxylase activities in the homogenates from the AdPGRMC1-infected cells were significantly lower than those in control (AdGFP-infected cells). In contrast, the chlorzoxazone 6-hydroxylase activity was not affected by the overexpression of PGRMC1 (Fig. 5B). These results suggest that PGRMC1 modulates the endogenous human P450 activity in an isoform-specific manner, supporting the results from the expression systems.

Coimmunoprecipitation of PGRMC1 and P450s. To investigate whether PGRMC1 directly interacts with P450s, we used a coimmunoprecipitation assay. Because commercially available antibodies against PGRMC1 or P450s are not suitable for immunoprecipitation assays, we constructed FLAG-PGRMC1 and Myc-P450 coexpression systems to perform the immunoprecipitation assay using anti-tag antibodies. We confirmed, by Western blot analyses using anti-FLAG and anti-c-Myc antibodies, that both FLAG-PGRMC1 and Myc-P450s were successfully expressed (Fig. 6). When the lysates using buffer A were assayed, the PGRMC1 in the three expression systems

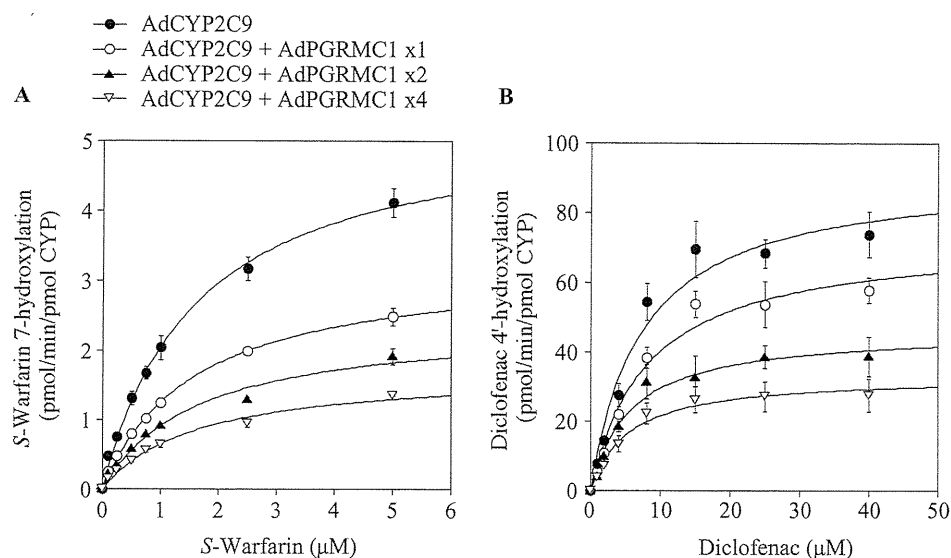


Fig. 3. Kinetic analyses of *S*-warfarin 7-hydroxylation (A) and diclofenac 4'-hydroxylation (B) by recombinant CYP2C9 in single or coexpression systems with PGRMC1. The expression systems were constructed using recombinant adenoviruses as described under *Materials and Methods*. The obtained kinetic parameters are shown in Table 3. Data are the means \pm S.D. of three independent determinations.

TABLE 3

Kinetic parameters for *S*-warfarin 7-hydroxylase activity and diclofenac 4'-hydroxylase activity by recombinant CYP2C9 in single or coexpression systems with PGRMC1

The expression systems were constructed using recombinant adenoviruses as described under *Materials and Methods*. Kinetic parameters were calculated from curves by nonlinear regression. Data are mean \pm S.D. of three independent experiments.

AdCYP2C9 + AdPGRMC1	<i>S</i> -Warfarin 7-Hydroxylation			Diclofenac 4'-Hydroxylation		
	K_m μM	V_{max} $\text{pmol} \cdot \text{min}^{-1} \cdot \text{pmol P450}^{-1}$	V_{max}/K_m $\mu\text{l} \cdot \text{min}^{-1} \cdot \text{pmol P450}^{-1}$	K_m μM	V_{max} $\text{pmol} \cdot \text{min}^{-1} \cdot \text{pmol P450}^{-1}$	V_{max}/K_m $\mu\text{l} \cdot \text{min}^{-1} \cdot \text{pmol P450}^{-1}$
×1	1.6 \pm 0.1	5.4 \pm 0.2	3.3 \pm 0.2	7.3 \pm 0.3	91.6 \pm 6.8	12.6 \pm 1.5
×2	1.6 \pm 0.1	3.3 \pm 0.2*	2.0 \pm 0.1*	8.1 \pm 0.5	72.9 \pm 4.7*	9.0 \pm 0.5*
×4	1.7 \pm 0.2	2.4 \pm 0.2**	1.5 \pm 0.1**	7.1 \pm 2.7	52.5 \pm 15.5**	7.5 \pm 0.5**
×4	1.7 \pm 0.2	1.7 \pm 0.1**	1.0 \pm 0.1**	8.4 \pm 0.6	42.2 \pm 6.7**	5.0 \pm 0.5**

* $P < 0.05$ and ** $P < 0.01$ compared with control by Shirley-Williams' test.

was immunoprecipitated to the same extent by using the anti-FLAG antibody, and only Myc-CYP2E1 was coimmunoprecipitated (Fig. 6A). When the lysates using buffer B were assayed, all three P450s were coimmunoprecipitated (Fig. 6B). These results suggest that PGRMC1 binds directly to these P450s, although the degree would be different among the isoforms.

Relationship between P450 Activities and PGRMC1, CPR, and Cytochrome b_5 Levels in a Panel of 29 Human Liver Microsomes. The midazolam 1'-hydroxylase, *S*-warfarin 7-hydroxylase, and chlorzoxazone 6-hydroxylase activities in a panel of 29 human liver microsomes were measured at the substrate concentrations of 10, 5, and 500 μM , and the PGRMC1, CYP3A4, CYP2C9, CYP2E1, CPR, and cytochrome b_5 protein levels were determined by Western blot analysis. The variability of the PGRMC1 protein levels was \sim 5-fold (Table 5). Although the variability of the CYP3A4 protein levels was large (3–72 pmol/mg, 24-fold), those of the CYP2C9 (5–17 pmol/mg, \sim 3-fold) and the CYP2E1 (3–16 pmol/mg, \sim 5-fold) protein levels were relatively small. As shown in Supplemental Fig. 1, A–C, the midazolam 1'-hydroxylase, *S*-warfarin 7-hydroxylase, and chlorzoxazone 6-hydroxylase activities represented as the metabolite $\cdot \text{min}^{-1} \cdot \text{mg protein}^{-1}$ were significantly correlated with CYP3A4, CYP2C9, and CYP2E1, respectively. To investigate whether the PGRMC1 would be a factor modulating the P450 activities, correlation analyses between the ratio of PGRMC1 to P450 and the midazolam 1'-hydroxylase, *S*-warfarin 7-hydroxylase, and chlorzoxazone 6-hydroxylase activities represented as the metabolite $\text{min}^{-1} \cdot \text{pmol P450}^{-1}$ were performed. We expected inverse correlations between PGRMC1/CYP3A4 ratio and midazolam 1'-hydroxylase or PGRMC1/CYP2C9

ratio and *S*-warfarin 7-hydroxylase activities based on the results of the coexpression systems in HepG2 cells. However, no inverse correlation was observed (Supplemental Fig. 1, D–F). In addition, except for the CPR/CYP2E1 ratio, the CPR/P450 or cytochrome b_5 /P450 ratios did not show a positive correlation with the activities (Supplemental Fig. 1, G–L). Next, we determined the relationship between the PGRMC1 protein level, and each P450 activity corrected with the CPR protein (Supplemental Fig. 2, A–C) or cytochrome b_5 protein (Supplemental Fig. 2, D–F) levels. However, no inverse correlation was observed in the CYP3A4 or CYP2C9 activities. Because the PGRMC1 protein levels were significantly correlated with the CPR ($r = 0.50$, $P < 0.01$) and cytochrome b_5 ($r = 0.76$, $P < 0.0001$) protein levels (Supplemental Fig. 2, G and H), it would be difficult to estimate the contribution of PGRMC1 to the P450 activities in HLM by the correlation analyses.

Discussion

In this study, we investigated the effects of PGRMC1 on the human drug-metabolizing P450 activities, focusing on three major isoforms, CYP3A4, CYP2C9, and CYP2E1. Using coexpression systems for PGRMC1/P450s in HepG2 cells, we found that PGRMC1 increased the K_m and decreased the V_{max} of the CYP3A4 activities and decreased the V_{max} of the CYP2C9 activities irrespective of the substrates (Figs. 2 and 3). In contrast to CYP3A4 and CYP2C9, PGRMC1 did not dramatically affect the CYP2E1 activities, indicating the effects of PGRMC1 would be P450 isoform dependent. During the process of preparing this report, an independent study reported that PGRMC1 commonly decreased the CYP3A4, CYP2C8, and rabbit

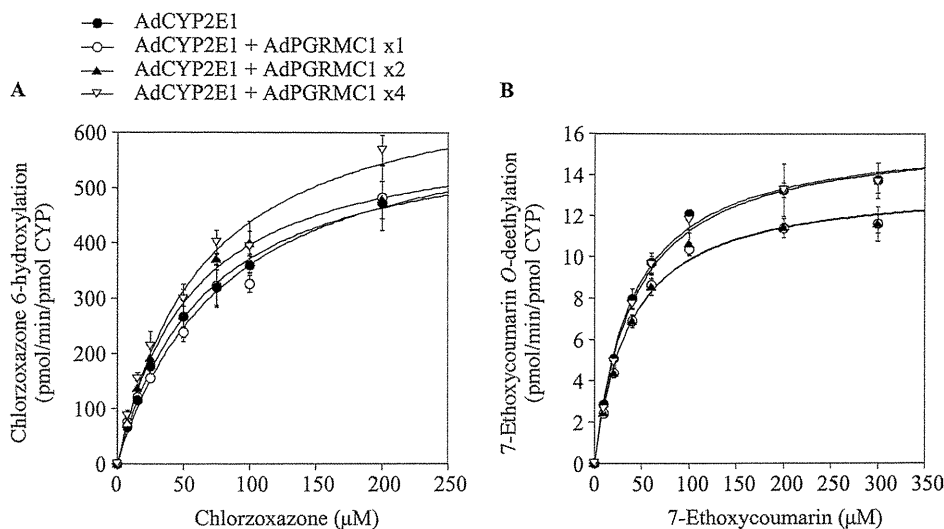


Fig. 4. Kinetic analyses of chlorzoxazone 6-hydroxylation (A) and 7-ethoxycoumarin O-deethylation (B) by recombinant CYP2E1 in single or coexpression systems with PGRMC1. The expression systems were constructed using recombinant adenoviruses as described under *Materials and Methods*. The obtained kinetic parameters are shown in Table 4. Data are the means \pm S.D. of three independent determinations.

TABLE 4

Kinetic parameters for chlorzoxazone 6-hydroxylase activity and 7-ethoxycoumarin O-deethylase activity by recombinant CYP2E1 in single or coexpression systems with PGRMC1

The expression systems were constructed using recombinant adenoviruses as described under *Materials and Methods*. Kinetic parameters are calculated from curves by nonlinear regression. Data are mean \pm S.D. of three independent experiments.

AdCYP2E1 + AdPGRMC1	Chlorzoxazone 6-Hydroxylation			7-Ethoxycoumarin O-Deethylation		
	K_m	V_{max}	V_{max}/K_m	K_m	V_{max}	V_{max}/K_m
	μM	$pmol \cdot min^{-1} \cdot pmol P450^{-1}$	$\mu l \cdot min^{-1} \cdot pmol P450^{-1}$	μM	$pmol \cdot min^{-1} \cdot pmol P450^{-1}$	$\mu l \cdot min^{-1} \cdot pmol P450^{-1}$
	67.1 ± 5.6	618.3 ± 18.2	9.3 ± 0.5	40.2 ± 2.5	16.0 ± 1.2	0.40 ± 0.01
×1	85.5 ± 21.6	667.8 ± 112.7	8.0 ± 0.8	38.3 ± 0.6	13.6 ± 0.4	$0.35 \pm 0.02^*$
×2	56.1 ± 8.2	617.9 ± 56.1	11.1 ± 0.6	38.3 ± 0.8	13.6 ± 0.7	$0.36 \pm 0.01^*$
×4	65.6 ± 7.2	723.1 ± 52.6	11.1 ± 1.0	42.6 ± 1.5	16.0 ± 0.4	$0.38 \pm 0.02^*$

* $P < 0.05$ compared with control by Shirley-Williams' test.

CYP2C2 activities using coexpression systems in HEK293 cells (Szczesna-Skorupa and Kemper, 2011). They evaluated the enzyme activities by P450-Glo assay at a substrate concentration. The findings that PGRMC1 decreased the activities of drug-metabolizing P450s were similar between our and recent reports, but our new findings are that the effects of PGRMC1 on the kinetics were different between the P450 isoforms and that there exists a P450(s) not affected by PGRMC1. When we mixed the homogenates from the single expression system for PGRMC1 and the homogenates from the single expression system for P450s, no changes were observed in the kinetics of each P450 activity (data not shown). Therefore, it was suggested that colocalization on the membrane would be critical for PGRMC1 to exert its effect in modulating the P450 activities. It has been reported that PGRMC1 is predominantly located in the endoplasmic reticulum. However, in a human ovarian cancer cell line, Ovar-3, PGRMC1 is found in the cytoplasm (Lösel et al., 2008). To analyze the localization of PGRMC1 in human liver, we performed Western blot analysis using cytosol, but PGRMC1 could not be detected. Therefore, the subcellular localization of PGRMC1 appears to be cell-type specific.

To investigate whether PGRMC1 modulates the activities of endogenous P450, we performed experiments using human hepatocytes. First, we sought to investigate the effects of repression of PGRMC1 by siRNA on the P450 activities (data not shown). When siRNA for PGRMC1 (Stealth select RNAi; Invitrogen) was transfected into human hepatocytes, the PGRMC1 mRNA levels were decreased by 70%. However, the PGRMC1 protein level was not decreased (data not shown). Although we used additional siRNA for PGRMC1 from another supplier (Ambion, Austin, TX), favorable results were not obtained. Hence, we sought to investigate the effects of the overex-

pression of PGRMC1 in human hepatocytes. The overexpression of PGRMC1 resulted in decreases in the CYP3A4 and CYP2C9 activities, but not CYP2E1 activity, which were the same as with the HepG2 coexpression systems (Fig. 5). These results suggest that PGRMC1 modulates the activities of endogenous P450 in an isoform-specific manner.

Using the coimmunoprecipitation assay (Fig. 6), we found that PGRMC1 interacts with P450s (not only CYP3A4 and CYP2C9 but also CYP2E1). When buffer A containing Nonidet P-40 and sodium deoxycholate, which are relatively strong detergents, was used, only CYP2E1 was coimmunoprecipitated (Fig. 6A). However, when buffer B containing digitonin, which is a relatively weaker detergent, was used, all of the three P450 isoforms were coimmunoprecipitated (Fig. 6B). These results suggested that the binding of PGRMC1 to CYP2E1 might be stronger than the binding to CYP3A4 or CYP2C9. Alternatively, the number of CYP2E1 molecules that bound to a PGRMC1 molecule might be larger than that of CYP3A4 or CYP2C9. In other words, a smaller number of PGRMC1 molecules may bind to CYP2E1. Such differences might explain why PGRMC1 did not affect the CYP2E1 activity but decreased the CYP3A4 and CYP2C9 activities, or the effects of PGRMC1 might not be a simple protein-protein interaction.

It was demonstrated that introduction of a mutation in the cytochrome b_5 -like domain of PGRMC1, to which heme binds, abolishes the binding to CYP7A1 (Mansouri et al., 2008). Min et al. (2005) also reported that a heme-deficient PGRMC1 mutant could not increase the CYP21A2 activity. These observations suggest the importance of heme binding for PGRMC1 in its function. Cytochrome b_5 has a hexacoordinate heme that is capable of transferring an electron. Mean-

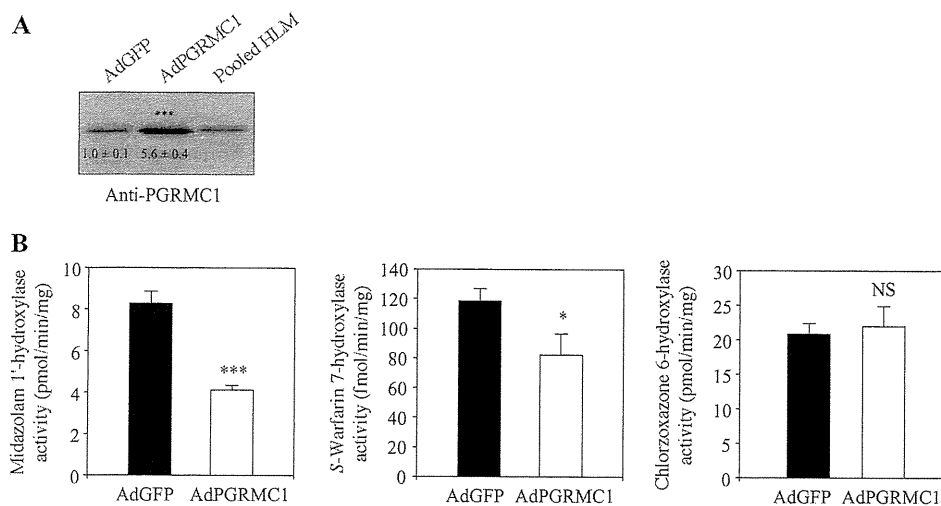


Fig. 5. Effects of overexpression of PGRMC1 on P450 activities in human hepatocytes. Human hepatocytes were infected with Ad-PGRMC1 or AdGFP at MOI 30. After 48 h, cells were collected and total cell homogenates were prepared. A, expression level of PGRMC1 in the homogenates (10 μg) was determined by Western blot analysis. Pooled HLMs (20 μg) were also subjected. B, midazolam 1'-hydroxylase activity (at 10 μM substrate concentration), S-warfarin 7-hydroxylase activity (at 10 μM substrate concentration), and chlorzoxazone 6-hydroxylase activity (at 500 μM substrate concentration) in the homogenates were measured. *, $P < 0.05$; ***, $P < 0.001$. NS, not significant.

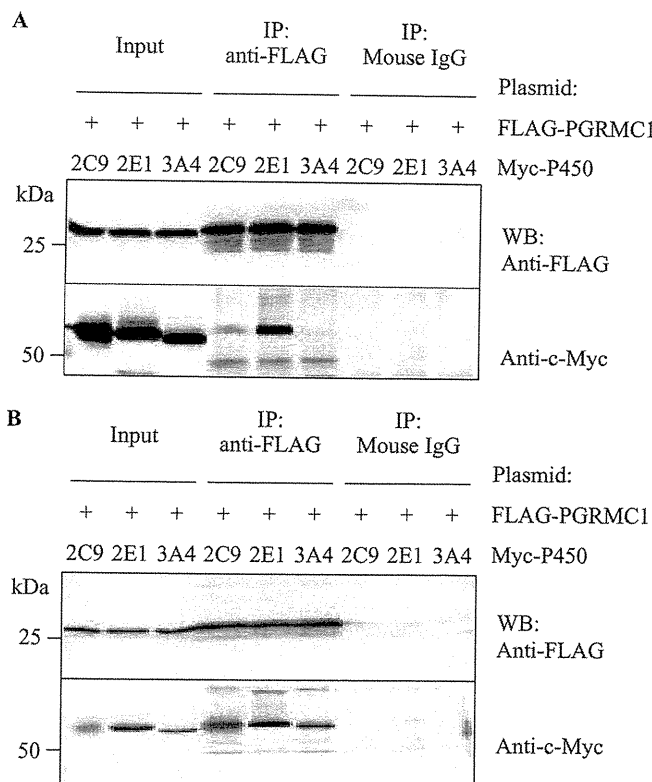


Fig. 6. Coimmunoprecipitation of FLAG-PGRMC1 and Myc-P450. FLAG-PGRMC1 plasmid and Myc-P450 (CYP3A4, CYP2C9, and CYP2E1) plasmid were transiently cotransfected into HEK293 cells. Five hundred micrograms of protein of the total cell homogenates were solubilized with buffer A (A) or buffer B (B) and immunoprecipitated with anti-FLAG antibody. The immunoprecipitates were subjected to SDS-PAGE followed by Western blot analyses using the anti-FLAG antibody or anti-Myc antibody. Input proteins (20 μ g) were also subjected to Western blot. Data are representative of at least three independent experiments. IP, immunoprecipitation; WB, Western blot.

while, PGRMC1 has a pentacoordinate heme (Cahill, 2007; Rohe et al., 2009), suggesting that PGRMC1 does not donate electrons to P450. Therefore, PGRMC1 affects the P450 function without direct electron transfer. Szczesna-Skorupa and Kemper (2011) reported that the PGRMC1-dependent inhibition of P450 activities is partially restored by the overexpression of CPR. In addition, because the coimmunoprecipitation of CPR and PGRMC1 was observed, they concluded that PGRMC1 binds to CPR and decreases the P450 activities. In contrast to their study, the coimmunoprecipitation of CPR and PGRMC1 was not observed in our system using HEK293 cells without the overexpression of CPR, probably because of the low expression level (data not shown). Alternatively, we measured the cytochrome *c* reduction and found that PGRMC1 did not alter the CPR activity (Supplemental Table 1). Thus, the decrease in the P450

activities by PGRMC1 might not be due to the decrease in CPR activity, although the possibility that PGRMC1 might influence the electron transferring from CPR to P450, because the V_{max} values of CYP3A4 and CYP2C9 were decreased, could not be excluded. In the case of CYP3A4, an increase in the K_m values was also observed. Therefore, as another mechanism, it is suggested that PGRMC1 might cause an allosteric change in the CYP3A4 structure that affects the affinity to substrates. Nevertheless, the effects of PGRMC1 on the P450 activity were diverse depending on the P450 isoforms, and further detailed studies are needed to clarify the underlying mechanisms.

In this study, the variability of the PGRMC1 protein levels in HLM was first evaluated. In 29 human liver samples, there was 5-fold variability (Table 5). We sought to estimate the contribution of PGRMC1 to the modulation of the P450 activities by correlation analyses between the P450 activities and P450 or PGRMC1 protein levels. In the analysis, we took into account the other components, the transferring of electrons to P450 such as CPR or cytochrome b_5 . Although these components positively regulate the enzyme activities of CYP3A4, CYP2C9, and CYP2E1, no clear correlation with the P450 activities was observed except in the case of CYP2E1. It has been reported that the molar ratio of P450/CPR/cytochrome b_5 seems to be important to understanding the role of CPR in the modulation of the P450 activities. We can determine the absolute expression levels of P450, CPR, and cytochrome b_5 but not PGRMC1. Understanding the absolute expression level of PGRMC1 in HLMs would be helpful to determine the relative importance of PGRMC1 in the modulation of the P450 activity.

Previous studies reported that PGRMC1 increased the activities of CYP21A2 and CYP51A1 that are responsible for steroid or sterol metabolism (Min et al., 2005; Hughes et al., 2007). In contrast, this study found that PGRMC1 decreased the activity of human drug-metabolizing P450s, which is supported in the study by Szczesna-Skorupa and Kemper (2011), although it is possibly isoform dependent. It has been reported that PGRMC1 is highly expressed in breast and ovary tumors and in cancer cell lines from the colon, thyroid, lung, and cervix (Crudden et al., 2005; Peluso et al., 2008a). Recently, it has been reported that PGRMC1 is highly expressed in human myometrium during pregnancy and may mediate the relaxation effect on myometrium (Wu et al., 2011). The changes of PGRMC1 expression under certain physiological conditions might impact on the metabolism of steroids. Meanwhile, little is known about the factors that affect the PGRMC1 expression level in human liver. Further studies are warranted to clarify the physiological significance of PGRMC1 in the modulation of drug-metabolizing P450 in liver.

In conclusion, we found that PGRMC1 decreases the activities of drug-metabolizing P450s in an isoform-dependent manner. The action was opposite to that for steroid-metabolizing P450s. Thus, PGRMC1 seems to affect P450s depending on their functions. The present study

TABLE 5

Expression levels of PGRMC1, P450s, CPR, and cytochrome b_5 and enzyme activities in human liver microsomes

Mean \pm S.D. and range of each value from 29 individual human liver microsomes are shown. Data are the mean of duplicate determinations.

	Relative Expression Level			Expression Level			Enzyme Activity		
	PGRMC1 ^a	CPR ^b	Cyt b_5 ^b	CYP3A4	CYP2C9	CYP2E1	MDZ	S-War	CZX
				pmol/mg			nmol \cdot min ⁻¹ \cdot mg ⁻¹		
Mean \pm S.D.	0.62 \pm 0.25	1.9 \pm 0.3	2.8 \pm 1.4	28 \pm 20	9 \pm 3	9 \pm 4	2.4 \pm 2.1	2.1 \pm 1.3	1.6 \pm 0.7
Range	0.23–1.23	1.0–2.6	1.0–6.3	3–72	5–17	3–16	0.1–8.5	0.5–5.6	0.7–3.6

Cyt b_5 , cytochrome b_5 ; MDZ, midazolam 1'-hydroxylase activity; S-war, S-warfarin 7-hydroxylase activity; CZX, chlorzoxazone 6-hydroxylase activity.

^a PGRMC1 protein level was expressed as relative to the pooled HLMs set at 1.0.

^b CPR and cytochrome b_5 protein levels are indicated as relative to the lowest set at 1.0.

revealed a novel function of PGRMC1 in modulating the drug-metabolizing activity.

Acknowledgments

We acknowledge Brent Bell for reviewing this manuscript.

Authorship Contributions

Participated in research design: Oda, Nakajima, Fukami, and Yokoi.

Conducted experiments: Oda.

Contributed new reagents or analytic tools: Oda, Toyoda, and Fukami.

Performed data analysis: Oda and Nakajima.

Wrote or contributed to the writing of the manuscript: Oda, Nakajima, and Yokoi.

References

- Cahill MA (2007) Progesterone receptor membrane component 1: an integrative review. *J Steroid Biochem Mol Biol* **105**:16–36.
- Crudden G, Loesel R, and Craven RJ (2005) Overexpression of the cytochrome p450 activator hpr6 (heme-1 domain protein/human progesterone receptor) in tumors. *Tumour Biol* **26**:142–146.
- Debose-Boyd RA (2007) A helping hand for cytochrome p450 enzymes. *Cell Metab* **5**:81–83.
- Ghosh K, Thompson AM, Goldbeck RA, Shi X, Whitman S, Oh E, Zhiwu Z, Vulpe C, and Holman TR (2005) Spectroscopic and biochemical characterization of heme binding to yeast Dap1p and mouse PGRMC1p. *Biochemistry* **44**:16729–16736.
- Guengerich FP (2002) Rate-limiting steps in cytochrome P450 catalysis. *Biol Chem* **383**:1553–1564.
- Hosomi H, Akai S, Minami K, Yoshikawa Y, Fukami T, Nakajima M, and Yokoi T (2010) An in vitro drug-induced hepatotoxicity screening system using CYP3A4-expressing and γ -glutamylcysteine synthetase knockdown cells. *Toxicol In Vitro* **24**:1032–1038.
- Hughes AL, Powell DW, Bard M, Eckstein J, Barbuch R, Link AJ, and Espenshade PJ (2007) Dap1/PGRMC1 binds and regulates cytochrome P450 enzymes. *Cell Metab* **5**:143–149.
- Iwamura A, Fukami T, Hosomi H, Nakajima M, and Yokoi T (2011) CYP2C9-mediated metabolic activation of losartan detected by a highly sensitive cell-based screening assay. *Drug Metab Dispos* **39**:838–846.
- Katoh M, Matsui T, Nakajima M, Tateno C, Kataoka M, Soeno Y, Horie T, Iwasaki K, Yoshizato K, and Yokoi T (2004) Expression of human cytochromes P450 in chimeric mice with humanized liver. *Drug Metab Dispos* **32**:1402–1410.
- Kronbach T, Mathys D, Umeno M, Gonzalez FJ, and Meyer UA (1989) Oxidation of midazolam and triazolam by human liver cytochrome P450IIIA4. *Mol Pharmacol* **36**:89–96.
- Laird SM, Vinson GP, and Whitehouse BJ (1988) Monoclonal antibodies against rat adrenocortical cell antigens. *Acta Endocrinol (Copenh)* **119**:420–426.
- Locuson CW, Gannett PM, and Tracy TS (2006) Heteroactivator effects on the coupling and spin state equilibrium of CYP2C9. *Arch Biochem Biophys* **449**:115–129.
- Lösel RM, Besong D, Peluso JJ, and Wehling M (2008) Progesterone receptor membrane component 1—many tasks for a versatile protein. *Steroids* **73**:929–934.
- Mansouri MR, Schuster J, Badhai J, Stattin EL, Lösel R, Wehling M, Carlsson B, Hovatta O, Karlström PO, Golovleva I, et al. (2008) Alterations in the expression, structure and function of progesterone receptor membrane component-1 (PGRMC1) in premature ovarian failure. *Hum Mol Genet* **17**:3776–3783.
- Mifsud W and Bateman A (2002) Membrane-bound progesterone receptors contain a cytochrome b_5 -like ligand-binding domain. *Genome Biol* **3**:RESEARCH0068.
- Min L, Takemori H, Nonaka Y, Katoh Y, Doi J, Horike N, Osamu H, Raza FS, Vinson GP, and Okamoto M (2004) Characterization of the adrenal-specific antigen IZA (inner zone antigen) and its role in the steroidogenesis. *Mol Cell Endocrinol* **215**:143–148.
- Min L, Strushkevich NV, Harnastai IN, Iwamoto H, Gilep AA, Takemori H, Usanov SA, Nonaka Y, Hori H, Vinson GP, et al. (2005) Molecular identification of adrenal inner zone antigen as a heme-binding protein. *FEBS J* **272**:5832–5843.
- Mohri T, Nakajima M, Fukami T, Takamiya M, Aoki Y, and Yokoi T (2010) Human CYP2E1 is regulated by miR-378. *Biochem Pharmacol* **79**:1045–1052.
- Nakajima M, Nakamura S, Tokudome S, Shimada N, Yamazaki H, and Yokoi T (1999) Azelastine N-demethylation by cytochrome P-450 (CYP)3A4, CYP2D6, and CYP1A2 in human liver microsomes: evaluation of approach to predict the contribution of multiple CYPs. *Drug Metab Dispos* **27**:1381–1391.
- Nebert DW and Russell DW (2002) Clinical importance of the cytochromes P450. *Lancet* **360**:1155–1162.
- Nelson DR, Zeldin DC, Hoffman SM, Maltais LJ, Wain HM, and Nebert DW (2004) Comparison of cytochrome P450 (CYP) genes from the mouse and human genomes, including nomenclature recommendations for genes, pseudogenes and alternative-splice variants. *Pharmacogenetics* **14**:1–18.
- Peluso JJ, Liu X, Saunders MM, Claffey KP, and Phoenix K (2008a) Regulation of ovarian cancer cell viability and sensitivity to cisplatin by progesterone receptor membrane component-1. *J Clin Endocrinol Metab* **93**:1592–1599.
- Peluso JJ, Romak J, and Liu X (2008b) Progesterone receptor membrane component-1 (PGRMC1) is the mediator of progesterone's antiapoptotic action in spontaneously immortalized granulosa cells as revealed by PGRMC1 small interfering ribonucleic acid treatment and functional analysis of PGRMC1 mutations. *Endocrinology* **149**:534–543.
- Rohe HJ, Ahmed IS, Twist KE, and Craven RJ (2009) Progesterone receptor membrane component 1: a targetable protein with multiple functions in steroid signaling, P450 activation and drug binding. *Pharmacol Ther* **121**:14–19.
- Shimada T, Yamazaki H, Mimura M, Inui Y, and Guengerich FP (1994) Interindividual variations in human liver cytochrome P-450 enzymes involved in the oxidation of drugs, carcinogens and toxic chemicals: studies with liver microsomes of 30 Japanese and 30 Caucasians. *J Pharmacol Exp Ther* **270**:414–423.
- Szczesna-Skorupa E and Kemper B (2011) Progesterone receptor membrane component 1 inhibits the activity of drug-metabolizing cytochromes P450 and binds to cytochrome P450 reductase. *Mol Pharmacol* **79**:340–350.
- Tabata T, Katoh M, Tokudome S, Hosakawa M, Chiba K, Nakajima M, and Yokoi T (2004) Bioactivation of capecitabine in human liver: involvement of the cytosolic enzyme on 5'-deoxy-5-fluorocytidine formation. *Drug Metab Dispos* **32**:762–767.
- Wu W, Shi SQ, Huang HJ, Balducci J, and Garfield RE (2011) Changes in PGRMC1, a potential progesterone receptor, in human myometrium during pregnancy and labour at term and preterm. *Mol Hum Reprod* **17**:233–242.
- Yamazaki H, Gillam EM, Dong MS, Johnson WW, Guengerich FP, and Shimada T (1997) Reconstitution of recombinant cytochrome P450 2C10(2C9) and comparison with cytochrome P450 3A4 and other forms: effects of cytochrome P450–P450 and cytochrome P450– b_5 interactions. *Arch Biochem Biophys* **342**:329–337.
- Yamazaki H, Tanaka M, and Shimada T (1999) Highly sensitive high-performance liquid chromatographic assay for coumarin 7-hydroxylation and 7-ethoxycoumarin O-deethylation by human liver cytochrome P450 enzymes. *J Chromatogr B Biomed Sci Appl* **721**:13–19.

Address correspondence to: Dr. Tsuyoshi Yokoi, Drug Metabolism and Toxicology, Faculty of Pharmaceutical Sciences, Kanazawa University, Kakumachi, Kanazawa 920-1192, Japan. E-mail: tyokoi@kenroku.kanazawa-u.ac.jp

Supplemental Data

Progesterone receptor membrane component 1 modulates human cytochrome P450 activities in an isoform-dependent manner

Shingo Oda, Miki Nakajima, Yasuyuki Toyoda, Tatsuki Fukami, and Tsuyoshi Yokoi

Drug Metabolism and Disposition

Material and Methods

CPR Activity. CPR activities in the co-expression systems of PGRMC1 and P450 in HepG2 cells were measured spectrophotometrically at 550 nm. Cytochrome *c* (Wako Pure Chemical Industries), reduced by CPR in the presence of NADPH, has a chromophore that absorbs visible light at 550 nm with $\epsilon = 21,000 \text{ M}^{-1}\text{cm}^{-1}$. Reactions were carried out in a cuvette containing 50 μM cytochrome *c*, 1 mM potassium cyanide, 0.35 M potassium phosphate buffer (pH 7.4), 100 μg of the co-expression system (Fig. 1), and 42 μM NADPH in a final volume of 1 mL. Reactions were initiated by the addition of NADPH, and the change in $A_{550 \text{ nm}}$ was monitored at room temperature for 5 min. Data obtained were shown to reflect initial reaction rates, representing three replicate assays for each sample.

Supplemental Table 1. CPR activity in the co-expression systems of PGRMC1 and P450s.

AdPGRMC1	CPR activity (nmol/min/mg)		
	CYP3A4	CYP2C9	CYP2E1
-	9.6 \pm 0.6	15.7 \pm 0.9	9.2 \pm 0.9
\times 1	10.9 \pm 0.5	12.0 \pm 0.8	10.6 \pm 0.6
\times 2	9.1 \pm 1.0	13.5 \pm 0.5	10.3 \pm 0.4
\times 4	9.1 \pm 1.0	12.9 \pm 0.4	13.6 \pm 0.5

The CPR activities in total cell homogenates from HepG2 cells overexpressing PGRMC1 and P450 were determined in cytochrome *c* reduction assays. The expression systems were constructed using recombinant adenoviruses as described under *Material and Methods*. Data are the mean \pm SD of triplicate determinations.

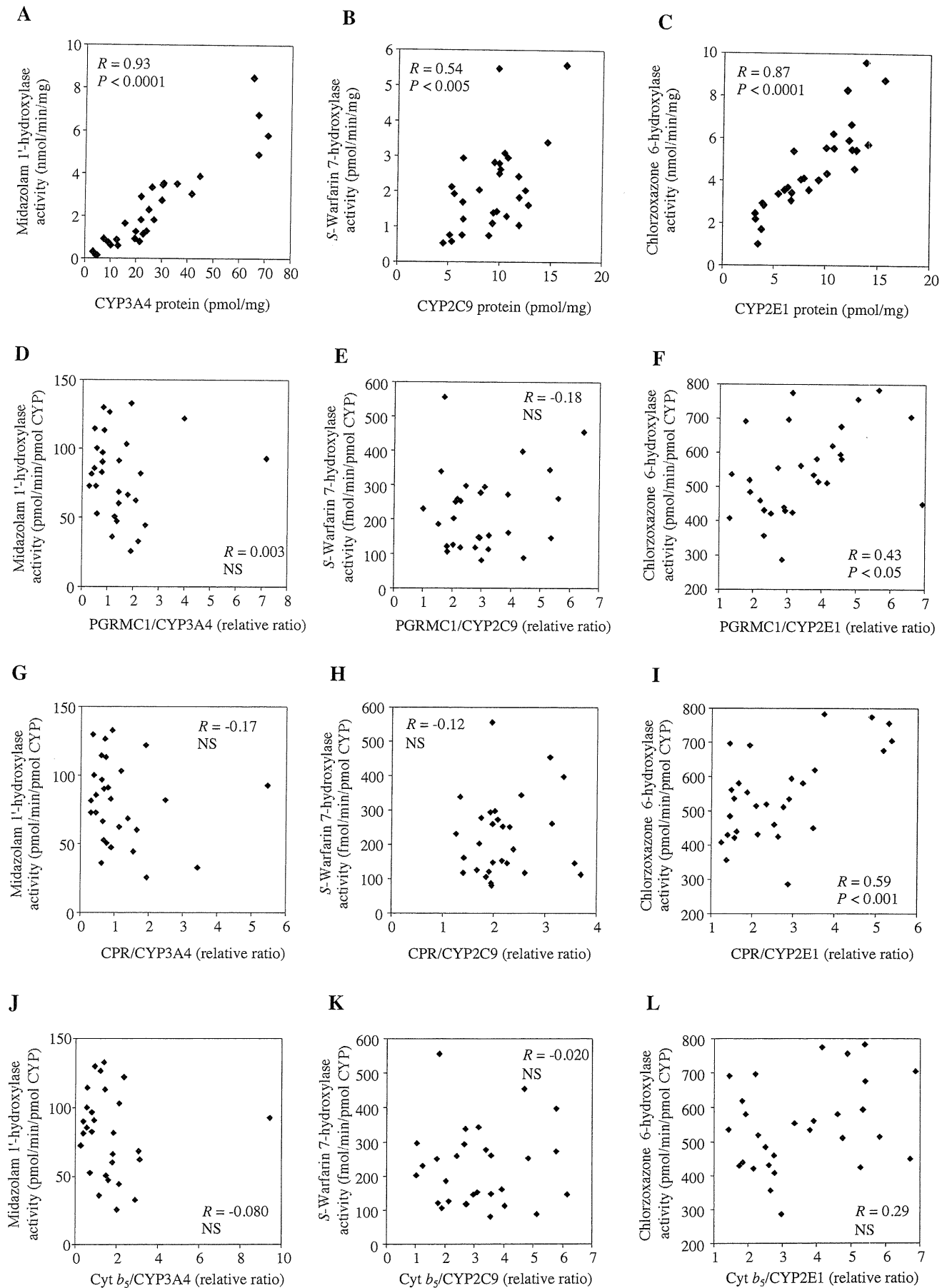
Supplemental Data

Progesterone receptor membrane component 1 modulates human cytochrome P450 activities in an isoform-depenedent manner

Shingo Oda, Miki Nakajima, Yasuyuki Toyoda, Tatsuki Fukami, and Tsuyoshi Yokoi
Drug Metabolism and Disposition

Supplemental figure 1. Scatter plots of midazolam 1'-hydroxylase, *S*-warfarin 7-hydroxylase, or chlorzoxazone 6-hydroxylase activities versus each P450 protein levels (A-C), and the ratio of PGRMC1 protein (D-F), CPR (G-I), or cytochrome *b*₅ (J-L) to each P450 protein in a panel of 29 human liver microsomes. Pearson's correlations (*R*) and corresponding *P* values are shown in the plot. Each data point is the mean of duplicate determinations. Cyt *b*₅, cytochrome *b*₅. NS, not significant.

Supplemental figure 1

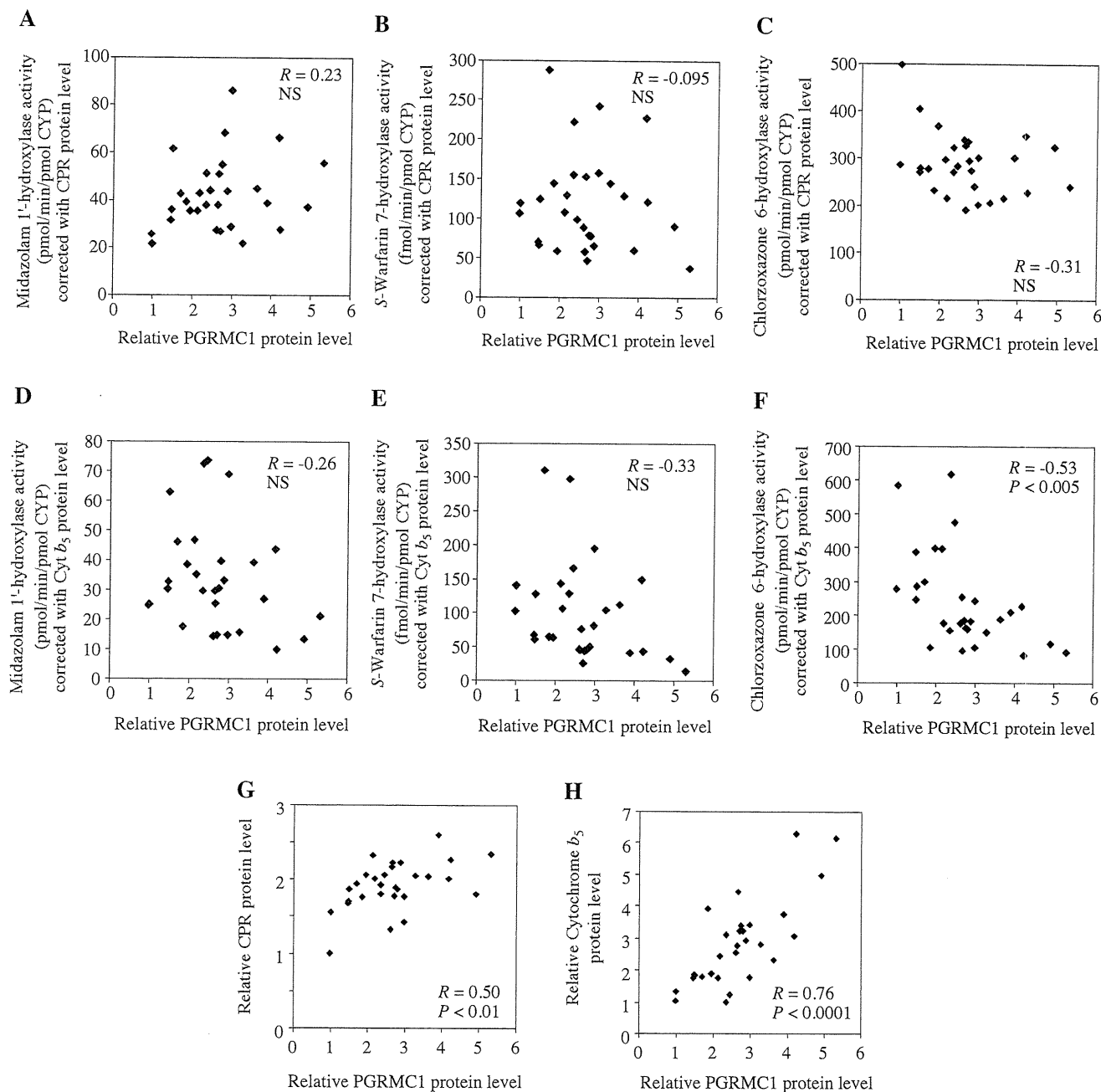


Supplemental Data

Progesterone receptor membrane component 1 modulates human cytochrome P450 activities in an isoform-dependent manner

Shingo Oda, Miki Nakajima, Yasuyuki Toyoda, Tatsuki Fukami, and Tsuyoshi Yokoi
Drug Metabolism and Disposition

Supplemental figure 2



Supplemental figure 2. Scatter plots of PGRMC1 protein levels versus midazolam 1'-hydroxylase, S-warfarin 7-hydroxylase, or chlorzoxazone 6-hydroxylase activities corrected with CPR protein level (A-C) or cytochrome b_5 (D-F), and versus CPR protein levels (G) or cytochrome b_5 protein levels (H) in a panel of 29 human liver microsomes. The PGRMC1, CPR, and cytochrome b_5 protein levels are expressed as relative value to the lowest set at 1. Pearson's correlations (R) and corresponding P values are shown in the plot. Each data point is the mean of duplicate determinations. Cyt b_5 , cytochrome b_5 . NS, not significant.

Mechanism of Exacerbative Effect of Progesterone on Drug-Induced Liver Injury

Yasuyuki Toyoda,* Shinya Endo,* Koichi Tsuneyama,† Taishi Miyashita,* Azusa Yano,* Tatsuki Fukami,* Miki Nakajima,* and Tsuyoshi Yokoi*¹

*Drug Metabolism and Toxicology, Faculty of Pharmaceutical Sciences, Kanazawa University, Kakuma-machi, Kanazawa 920-1192, Japan; and †Department of Diagnostic Pathology, Graduate School of Medicine and Pharmaceutical Science for Research, University of Toyama, Sugitani, Toyama 930-0194, Japan

¹To whom correspondence should be addressed. Fax: +81-76-234-4407. E-mail: tyokoi@kenroku.kanazawa-u.ac.jp.

Received August 23, 2011; accepted November 22, 2011

Drug-induced liver injury (DILI) is a major safety concern in drug development and clinical drug therapy. However, the underlying mechanism of DILI is little known. It is generally believed that women exhibit worse outcomes from DILI than men. Recently, we found that pretreatment of mice with estradiol attenuated halothane (HAL)-induced liver injury, whereas pretreatment with progesterone exacerbated it in female mice. To investigate the mechanism of sex difference of DILI, we focused on progesterone in this study. We found the exacerbating effect of progesterone in thioacetamide (TA), α -naphthylisothiocyanate, and dicloxacillin-induced liver injury only in female mice. Higher number of myeloperoxidase-positive mononuclear cells infiltrated into the liver and increased levels of Chemokine (C-X-C motif) ligand 1 and 2 (CXCL1 and CXCL2) and intercellular adhesion molecule-1 in the liver were observed. Interestingly, CXCL1 was slightly increased by progesterone pretreatment alone. Progesterone pretreatment increased the extracellular signal-regulated kinase (ERK) phosphorylation in HAL-induced liver injury. Pretreatment with U0126 (ERK inhibitor) significantly suppressed the exacerbating effect of progesterone and the expression of inflammatory mediators. In addition, pretreatment with gadolinium chloride (GdCl₃; inhibitor of Kupffer cells) significantly suppressed the exacerbating effect of progesterone pretreatment and the expression of inflammatory mediators. Moreover, post-treatment of RU486 (progesterone receptor antagonist) 1 h after the HAL or TA administration ameliorated the HAL- or TA-induced liver injury, respectively, in female mice. In conclusion, progesterone exacerbated the immune-mediated hepatotoxic responses in DILI via Kupffer cells and ERK pathway. The inhibition of progesterone receptor and decrease of the immune response may have important therapeutic implications in DILI.

Key Words: drug-induced liver injury; CXCL1; sex difference; Kupffer cell; progesterone receptor antagonist.

Drug-induced liver injury (DILI) is the most frequent reason for the withdrawal of an approved drug from the market and for failures in drug development in pharmaceutical companies. In most cases, the mechanisms of hepatotoxicity are not elucidated,

but it is likely to arise from complex interactions among drug properties, daily dose, genetic variations, age, sex, diseases, and environmental factors (Chalasan and Björnsson, 2010; Li, 2002). In general, women are more susceptible to liver injury by therapeutic drugs than men. Seventy-four percent of all acute liver failure cases are women (Miller, 2001). It has been reported that 78% of DILI cases are in women and a significantly greater number of women show DILI than men (Björnsson and Olsson, 2005; DeValle *et al.*, 2006; Ostapowicz *et al.*, 2002). Although some reports described that female sex is not a predisposing factor for DILI, it was also reported that patients with severe DILI who underwent liver transplantation were more frequently women (76%) and that nearly 90% of patients with fulminant liver injury from DILI were women (Andrade *et al.*, 2005; Lucena *et al.*, 2009; Russo *et al.*, 2004). From these lines of study, women appear to be at greater risk of developing severe liver injury, but it is not clear why women exhibit the worst outcomes from liver injury.

It has been reported that women elicit more vigorous cellular and humoral immune reactions and suffer in greater numbers from autoimmune disease than men (Ansar *et al.*, 1985; Ostensen, 1999). Moreover, immune-mediated diseases in women may be exacerbated during the reproductive phase (Ansar *et al.*, 1985; Ostensen, 1999). Circulating levels of estradiol (E2) and progesterone fluctuate as a result of the reproductive phase and pregnancy in females (Barkley *et al.*, 1979; Wood *et al.*, 2007). There is evidence that the immune system is regulated by circulating level of sex steroid hormones, E2, progesterone, and testosterone (Grossman, 1985). It was also reported that E2 decreased and progesterone increased the production of proinflammatory cytokines in oxidative stress-stimulated murine peritoneal macrophage and human mononuclear cells and their receptor antagonists, ICI 182,780 and RU486, blocked these effects, respectively (Huang *et al.*, 2008; Yuan *et al.*, 2008). Recently, there have been many reports that immune reactions may have a critical role in DILI and that hepatic inflammation determines the

extent of liver injury (Adams *et al.*, 2010; Deng *et al.*, 2009; Holt and Ju, 2006). However, there has been little information concerning the involvement of female sex hormones in DILI. There are some reports that E2-attenuated liver injury caused by ischemia-reperfusion, trauma-hemorrhage, and acetaminophen (APAP) (Chandrasekaran *et al.*, 2011; Shimizu *et al.*, 2008; Yokoyama *et al.*, 2005), but there is little information about the effect of progesterone in liver injury.

We recently reported that the progesterone pretreatment exacerbated the immune-mediated hepatotoxic responses in halothane (HAL)-induced liver injury in female mice (Toyoda *et al.*, 2011). In this study, we investigated the underlying mechanism of the progesterone-induced exacerbation of DILI using a mouse model.

MATERIALS AND METHODS

Materials. HAL was purchased from Takeda Yakuhin (Osaka, Japan) and Isoflurane (ISO) was from Abbott Japan (Tokyo, Japan). Progesterone, gadolinium chloride (GdCl₃), and dicloxacillin (DCX) were purchased from Sigma-Aldrich (St Louis, MO). Mifepristone (RU486) and α -naphthylisothiocyanate (ANIT) were from Tokyo Kasei (Tokyo, Japan). U0126, SB203580, and thioacetamide (TA) were from Wako Pure Chemical Industries (Osaka, Japan). SP600125 was from Calbiochem (Los Angeles, CA). ICI 182,780 (ICI) was from TOCRIS Bioscience (Ellisville, MO). Fuji Dri-Chem slides of GPT/ALT-PHII and GOT/AST-PHII to measure alanine aminotransferase (ALT)/glutamic pyruvic transaminase (GPT) and aspartate aminotransferase (AST)/glutamic oxaloacetic transaminase (GOT), respectively, were from Fuji Film Med. Co. (Tokyo, Japan). Rabbit polyclonal antibody against mouse myeloperoxidase (MPO) was from DAKO (Carpinteria, CA). Rat polyclonal antibody against F4/80 was from U.K.-Serotec (Oxford, U.K.). The monoclonal antibodies of anti-Thr202/Tyr204 phosphorylated extracellular signal-regulated kinase (ERK) 1/2, anti-Thr180/Tyr182 phosphorylated p38 mitogen-activated protein (MAP) kinase, and anti-Thr183/Tyr185 phosphorylated c-Jun N-terminal kinase (JNK) 1/2 were purchased from Cell Signaling Technology (Beverly, MA). The monoclonal antibodies against ERK1/2 and JNK1/2 and the polyclonal antibody against p38 MAP kinase were also from Cell Signaling Technology. All primers were commercially synthesized at Hokkaido System Sciences (Sapporo, Japan). All other chemicals were of the highest grade commercially available.

Animals. Female BALB/cCrSlc mice (8 weeks old, 20–25 g) were obtained from SLC Japan (Shizuoka, Japan). Animals were housed in a controlled environment (temperature 25 ± 1°C, humidity 50 ± 10%, and 12-h light/12-h dark cycle) in the institutional animal facility with access to food and water *ad libitum*. Animals were acclimatized for a week before use for the experiments. Animal maintenance and treatment were performed in accordance with the National Institutes of Health Guide for Animal Welfare of Japan, as approved by the Institutional Animal Care and Use Committee of Kanazawa University, Japan.

Administration of hepatotoxic compounds in progesterone-pretreated mice. The progesterone pretreatment methods were described previously (Toyoda *et al.*, 2011). In brief, female mice were pretreated with progesterone (0.3 mg/mouse, sc) for 7 days followed by the administration of HAL (15 or 30 mmol/kg, ip), TA (50 mg/kg, ip), ANIT (80 mg/kg, po), DCX (600 mg/kg, ip), or ISO (15 mmol/kg, ip) 1.5 h after the last treatment of progesterone. In the ANIT experiments, the mice were fasted for 15 h prior to the ANIT administration. Six hours after DCX administration and 24 h after HAL, TA, ANIT, or ISO administration, the mice were sacrificed, and the plasma and the liver were collected. The liver was fixed in buffered neutral 10% formalin and used for immunohistochemical staining. The degree of liver injury was assessed

by hematoxylin-eosin (H&E) staining, and the plasma AST and ALT levels were determined using Fuji Dri-Chem 4000V (Fuji Film Med. Co.). The mononuclear cells infiltration was assessed by immunostaining for MPO as previously described (Kumada *et al.*, 2004).

Administration of HAL in U0126- or GdCl₃-pretreated mice. Mice were pretreated with progesterone for 7 days. In experiments using ERK inhibitor, mice were treated with U0126 (ERK inhibitor, 10 mg/kg, ip) 1 h before the HAL administration (30 mmol/kg, ip). In experiments using an inhibitor of Kupffer cells, mice were treated with GdCl₃ (10 mg/kg, iv) 24 and 48 h before the HAL administration (30 mmol/kg, ip). Twenty-four hours after the HAL administration, the mice were sacrificed. It was reported that a 40–61% reduction of the number of Kupffer cells in the mouse liver tissue occurred when treated with GdCl₃ in this method (Mosher *et al.*, 2001).

Administration of RU486 and HAL in mice. Mice were pretreated with RU486 (progesterone receptor antagonist, 50 µg/mouse, sc) for 7 days followed by HAL administration (30 mmol/kg, ip) 1.5 h after the last RU486 treatment, according to the method described previously (Toyoda *et al.*, 2011). In the experiments of postadministration of RU486, mice were administered RU486 (1 mg/kg, iv) 1 h after the HAL administration (30 mmol/kg, ip). Twenty-four hours after the HAL administration, the mice were sacrificed.

Real-time reverse transcription PCR analysis. RNA from mouse liver was isolated using RNeasy according to the manufacturer's instructions. Tumor necrosis factor α (TNF α), Chemokine (C-X-C motif) ligand 1 and 2 (CXCL1 and CXCL2), intercellular adhesion molecule-1 (ICAM-1), and glyceraldehyde-3-phosphate dehydrogenase (GAPDH) were quantified by real-time reverse transcription (RT)PCR. The primer sequences used in this study are shown in Table 1. The RT process and real-time PCR were performed as described previously (Kobayashi *et al.*, 2009).

Enzyme-linked immunosorbent assay. The CXC chemokines, CXCL1 and CXCL2, in plasma were measured by Quantikine Mouse CXCL1/KC ELISA and Quantikine Mouse CXCL2/MIP-2 ELISA (R&D Systems, Minneapolis, MN), respectively, according to the manufacturer's instructions.

Immunoblot analysis. SDS-polyacrylamide gel electrophoresis and immunoblot analysis were performed according to Laemmli (1970). Whole liver homogenates (50 µg) were separated on 10% polyacrylamide gels and electrotransferred onto polyvinylidene difluoride membrane, Immobilon-P (Millipore Corporation, Billerica, MA). The membranes were probed with the monoclonal antibodies of anti-ERK1/2, anti-JNK1/2, anti p38 MAP kinase, anti-Thr202/Tyr204 phosphorylated ERK1/2, anti-Thr183/Tyr185 phosphorylated JNK1/2, and anti-Thr180/Tyr182 phosphorylated p38 MAP kinase and the corresponding fluorescent dye-conjugated second antibody. An Odyssey Infrared Imaging system (LI-COR Biosciences, Lincoln, NE) was used for the detection. The relative expression level was quantified using ImageQuant TL Image Analysis software (GE Healthcare, Little Chalfont, Buckinghamshire, U.K.).

TABLE 1
Sequence of Primers Used for Real-Time RT-PCR Analyses in This Study

Target	Primer	Sequence
TNF α	FP	5'-TGT CTC AGC CTC TTC TCA TTC C-3'
	RP	5'-TGA GGG TCT GGG CCA TAG AAC-3'
CXCL1	FP	5'-GAT TCA CCT CAA GAA CAT CCA GAG-3'
	RP	5'-GAA GCC AGC GTT CAC CAG AC-3'
CXCL2	FP	5'-AAG TTT GCC TTG ACC CTG AAG-3'
	RP	5'-ATC AGG TAC GAT CCA GGC TTC-3'
ICAM-1	FP	5'-CAA GGA GAT CAC ATT CAC GG-3'
	RP	5'-CTT CCA GGG AGC AAA ACA AC-3'

Note. FP, Forward primer; RP, Reverse primer.

Cell culture and progesterone treatment. The mouse macrophage cell line RAW264.7 was kindly provided by Dr K. Miyamoto (Kanazawa University, Japan). RAW264.7 was maintained in Dulbecco's Modified Eagle's Medium from Nissui Pharmaceutical (Tokyo, Japan) containing 10% fetal bovine serum (BioWhittaker, Walkersville, MD), 3% glutamine, and 16% sodium bicarbonate in a 5% CO₂ atmosphere at 37°C. RAW264.7 were seeded at a density of 1×10^5 cells/well in 24-well plates with the medium containing the indicated concentration of progesterone and then incubated at 37°C. In experiments using MAP kinase inhibitors, cells were treated with 1 μM of MAP kinase/ERK (MEK) 1/2 inhibitor U0126, p38 MAP kinase inhibitor SB203580, or JNK1/2 inhibitor SP600125. In other experiments, cells were treated with progesterone receptor antagonist RU486 or E2 antagonist ICI. After incubation, the cells were harvested, and total RNA was prepared using RNeasy according to the manufacturer's protocols.

Statistical analysis. Data are presented as mean ± SD. Comparison of the two groups was made with an unpaired two-tailed Student's *t*-test. Comparison of multiple groups was made with ANOVA followed by Dunnett or Tukey test. A value of $p < 0.05$ was considered statistically significant.

RESULTS

Effect of Progesterone Pretreatment on the Time-Dependent Changes of Plasma Transaminase Levels in HAL-Induced Liver Injury

To investigate the effects of progesterone pretreatment on the time-dependent changes of plasma transaminase levels in HAL-induced liver injury, mice pretreated with progesterone (0.3 mg/mouse, sc) were administered HAL (15 mmol/kg, ip), which resulted in a significant increase of the ALT and AST levels at 24 and 36 h after the HAL administration in female mice but not in male mice (Fig. 1A and Supplementary fig. 1A).

Effect of Progesterone Pretreatment on the Time-Dependent Changes of CXCL Chemokines in HAL-Induced Liver Injury

To investigate whether the changes in liver injury in mice pretreated with progesterone after HAL administration resulted in increases of chemokines, we measured the hepatic messenger RNA (mRNA) expression and serum protein levels of CXCL1 and CXCL2. The hepatic CXCL1 and CXCL2 mRNA levels were markedly increased at 3 and 24 h after HAL administration in progesterone-pretreated mice, respectively (Fig. 1B). Interestingly, progesterone pretreatment alone increased CXCL1 mRNA (4.1-fold) and serum protein (2.3-fold) (0 h point in Figs. 1B and C). CXCL1 expression in response to HAL administration peaked at an earlier time point compared with CXCL2 expression. The time-dependent changes of the mRNA and protein levels were similar in CXCL1 and CXCL2. Thus, changes of mRNA expression were mainly followed in the subsequent experiments.

Among male mice, there was no marked difference in the mRNA expression levels of CXCL1 and CXCL2 after HAL administration in progesterone-pretreated mice compared with vehicle-pretreated mice (Supplementary fig. 1B). As with HAL-induced liver injury, the time-dependent changes of the transaminase levels and mRNA levels of CXCL1 and CXCL2

were similar to those associated with TA-induced liver injury (Supplementary fig. 2).

Effects of Progesterone Pretreatment on Various Hepatotoxic Compound-Induced Liver Injury

To investigate the effects of progesterone pretreatment on various compounds, TA, ANIT, DCX, or ISO were administered to the progesterone-pretreated mice. Female mice pretreated with progesterone showed significantly increased ALT and AST levels after the administration of TA, ANIT, or DCX, but not ISO, compared with vehicle-pretreated mice (Fig. 2A). However, male mice showed no effects on the transaminase levels by the administration of TA or ANIT as well as HAL (Supplementary fig. 3). Histopathological changes demonstrated that progesterone pretreatment enhanced TA- or ANIT-induced hepatocyte degeneration and damage. In addition, immunohistochemical analyses with anti-MPO antibody demonstrated that progesterone pretreatment increased the number of MPO-positive cells infiltrated in liver at 24 h after TA or ANIT administration (Fig. 2B). There was no change in either the histopathology findings or the number of MPO-positive cells in the liver of mice pretreated with progesterone alone. As with HAL-induced liver injury, hepatic mRNA level of CXCL1 and CXCL2 was increased significantly by progesterone pretreatment after TA, ANIT, and DCX administration compared with vehicle-pretreated mice (Fig. 2C).

Effects of Progesterone Pretreatment on Activation of MAP Kinase-Signaling Pathway in HAL-Induced Liver Injury

MAP kinases, including ERK1/2, p38 MAP kinase, and JNK1/2, are important components for many intracellular signaling pathways. The phosphorylation of MAP kinases, which are required for the enzyme activity, activates signaling cascades, the downstream effects of which have been linked to the regulation of the inflammatory responses (DeFranco *et al.*, 1998). To clarify the role of the MAP kinase-signaling pathway in the liver after the HAL administration, the phosphorylation of ERK1/2, p38 MAP kinase, and JNK1/2 in liver were assessed by immunoblot analyses. Progesterone pretreatment alone significantly increased the phosphorylation of ERK in female mice but not in male mice (Fig. 3 and Supplementary fig. 4). The phosphorylation of ERK was also significantly increased in female mice by the HAL administration compared with control (Fig. 3). Progesterone pretreatment and HAL administration had no effect of the phosphorylation of p38 MAP kinase and JNK1/2 in female and male mice (data not shown).

Effects of ERK Pathway on Progesterone Pretreatment-Induced Exacerbation of HAL-Induced Liver Injury

To investigate whether the activation of the ERK pathway is involved in the progesterone pretreatment-induced exacerbation of liver injury, mice pretreated with progesterone were treated with an ERK inhibitor U0126, followed by the administration of